

LOCKHEED MARTIN ENERGY RESEARCH LIBRARIES

3 4456 0515479 3

CENTRAL RESEARCH LIBRARY
ORNL-4909
(ENDF-206)

Cy 1

**^{206}Pb , ^{207}Pb , AND ^{208}Pb NEUTRON
ELASTIC AND INELASTIC SCATTERING
CROSS SECTIONS FROM 5.50 TO 8.50 MeV**

W. E. Kinney
F. G. Perey

OAK RIDGE NATIONAL LABORATORY
CENTRAL RESEARCH LIBRARY
DOCUMENT COLLECTION
LIBRARY LOAN COPY
DO NOT TRANSFER TO ANOTHER PERSON
If you wish someone else to see this
document, send in name with document
and the library will arrange a loan.
UCN-7969
(S 3-67)



OAK RIDGE NATIONAL LABORATORY
OPERATED BY UNION CARBIDE CORPORATION • FOR THE U.S. ATOMIC ENERGY COMMISSION

Printed in the United States of America. Available from
National Technical Information Service
U.S. Department of Commerce
5285 Port Royal Road, Springfield, Virginia 22151
Price: Printed Copy \$5.45; Microfiche \$1.45

This report was prepared as an account of work sponsored by the United States Government. Neither the United States nor the United States Atomic Energy Commission, nor any of their employees, nor any of their contractors, subcontractors, or their employees, makes any warranty, express or implied, or assumes any legal liability or responsibility for the accuracy, completeness or usefulness of any information, apparatus, product or process disclosed, or represents that its use would not infringe privately owned rights.

ORNL-4909
UC-79d
(ENDF-206)

Contract No. W-7405-eng-26

Neutron Physics Division

^{206}Pb , ^{207}Pb , AND ^{208}Pb NEUTRON ELASTIC AND INELASTIC SCATTERING
CROSS SECTIONS FROM 5.50 TO 8.50 MeV

W. E. Kinney and F. G. Perey

JUNE 1974

OAK RIDGE NATIONAL LABORATORY
Oak Ridge, Tennessee 37830
operated by
UNION CARBIDE CORPORATION
for the
U.S. ATOMIC ENERGY COMMISSION

LOCKHEED MARTIN ENERGY RESEARCH LIBRARIES



3 4456 0515479 3

CONTENTS

Abstract	1
Introduction.....	1
Data Acquisition.....	1
Data Reduction	2
Results	4
Elastic Scattering Differential Cross Sections.....	4
Inelastic Scattering Differential Cross Sections.....	4
Excitation Functions	8
Inelastic Scattering to the Continuum.....	17
Conclusions.....	25
Acknowledgments.....	25
References.....	26
Appendix	28

^{206}Pb , ^{207}Pb , AND ^{208}Pb NEUTRON ELASTIC AND INELASTIC SCATTERING

CROSS SECTIONS FROM 5.50 TO 8.50 MeV

W. E. Kinney and F. G. Perey

ABSTRACT

Measured neutron ^{208}Pb differential elastic scattering cross sections at 5.50, 7.00, and 8.50 MeV are given and compared with previous results. Measured ^{206}Pb , ^{207}Pb , and ^{208}Pb neutron inelastic scattering cross sections are given at roughly 0.5 MeV intervals from 5.50 to 8.50 MeV and also compared with previous results. ENDF/B III MAT 1136 elastic angular distributions, angle integrated elastic and inelastic scattering cross sections, and nuclear temperatures are in generally good agreement with experiment over this energy range.

INTRODUCTION

The data reported here are the results of one of a series of experiments to measure neutron elastic and inelastic scattering cross sections at the ORNL Van de Graaffs. Reports in the series are listed in Reference 1. This report presents measured neutron elastic and inelastic scattering cross sections for ^{206}Pb , ^{207}Pb , and ^{208}Pb from 5.50 to 8.50 MeV. To assist in the evaluation of the data, the data acquisition and reduction techniques are first briefly discussed. For the purposes of discussion the data are presented in graphical form and are compared with the results of others and with ENDF/B III (Evaluated Neutron Data File B, Version III) MAT 1136(Ref. 2). Tables of numerical values of the elastic scattering cross sections and cross sections for inelastic scattering to discrete levels in the residual nucleus are given in an appendix.

DATA ACQUISITION

The data were obtained with conventional time-of-flight techniques. Pulsed (2 MHz), bunched (approximately 1.5 nsec full width at half maximum, FWHM) deuterons accelerated by the ORNL Van de Graaffs interacted with deuterium in a gas cell to produce neutrons by the $\text{D}(\text{d},\text{n})^3\text{He}$ reaction. The gas cells, of length 1 and 2 cm, were operated at pressures of approximately 1.5 atm and gave neutron energy resolutions of the order of ± 60 keV.

The neutrons were scattered from solid right circular cylindrical samples placed approximately 10 cm from the gas cells when the detector angles were greater than 25 degrees. For smaller detector angles the cell-to-sample distance had to be increased to 33 cm in order to shield the detectors from neutrons coming directly from the gas cells. The ^{206}Pb sample had a diameter of 1.60 cm, height of 3.10 cm, and mass of 59.0 gm. The ^{207}Pb sample was 2.00 cm in diameter, 1.90 cm in height, with a mass of 67.0 gm. The ^{208}Pb sample had a diameter of 2.00 cm, height of 3.80 cm, and a mass of 136.0 gm.

The scattered neutrons were detected by 12.5 cm diameter NE-213 liquid scintillators optically coupled to XP-1040 photomultipliers. The scintillators were 2.5 cm thick. Data were taken with three detectors simultaneously. Flight paths were approximately 4 m with the detector angles ranging from 15 to 140 degrees. The gas cell neutron production was monitored by a time-of-flight system which used a 5 cm diameter by 2.5 cm thick NE-213 scintillator viewed by a 56-AVP photomultiplier placed about 4 m from the cell at an angle of 55 degrees with the incident deuteron beam.

For each event a PDP-7 computer was given the flight time of a detected recoil proton event with reference to a beam pulse signal, the pulse height of the recoil proton event, and identification of the detector. The electronic equipment for supplying this information to the computer consisted, for the most part, of standard commercial components. The electronic bias was set at approximately 700 keV neutron energy to ensure good pulse shape discrimination against gamma-rays at all energies.

The detector efficiencies were measured by (n,p) scattering from a 6 mm diameter polyethylene sample and by detecting source $D(d,n)^3\text{He}$ neutrons at 0 degrees³. Both interactions gave results which agreed with each other and which yielded efficiency versus energy curves that compared well with calculations⁴.

DATA REDUCTION

Central to the data reduction process was the use of a light pen with the PDP-7 computer oscilloscope display programs to extract peak areas from spectra. The light pen made a comparatively easy job of estimating errors in the cross section caused by extreme but possible peak shapes.

The reduction process started by normalizing a sample-out to a sample-in time-of-flight spectrum by the ratio of their monitor neutron peak areas, subtracting the sample-out spectrum, and transforming the difference spectrum into a spectrum of center-of-mass cross section versus excitation energy. This transformation allowed ready comparison of spectra taken at different angles and incident neutron energies by removing kinematic effects. It also made all single peaks have approximately the same shape and width regardless of excitation energy (in a time-of-flight spectrum, single peaks broaden with increasing flight time). A spectrum of the variance based on the counting statistics of the initial data was also computed. Figure 1 shows a typical time-of-flight spectrum and its transformed energy spectrum.

The transformed spectra were read into the PDP-7 computer and the peak stripping was done with the aid of the light pen. A peak was stripped by drawing a background beneath it, subtracting the background, and calculating the area, centroid, and FWHM of the difference. The variance spectrum was used to compute a counting statistics variance corresponding to the stripped peak. Peak stripping errors due to uncertainties in the residual background under the peaks or to the tails of imperfectly resolved nearby peaks could be included with the other errors by stripping the peaks several times corresponding to high, low, and best estimates of this background. Although somewhat subjective, the low and high estimates of the cross sections were identified with 95% confidence limits; these, together with the best estimate, defined upper and lower errors due to stripping. When a spectrum was

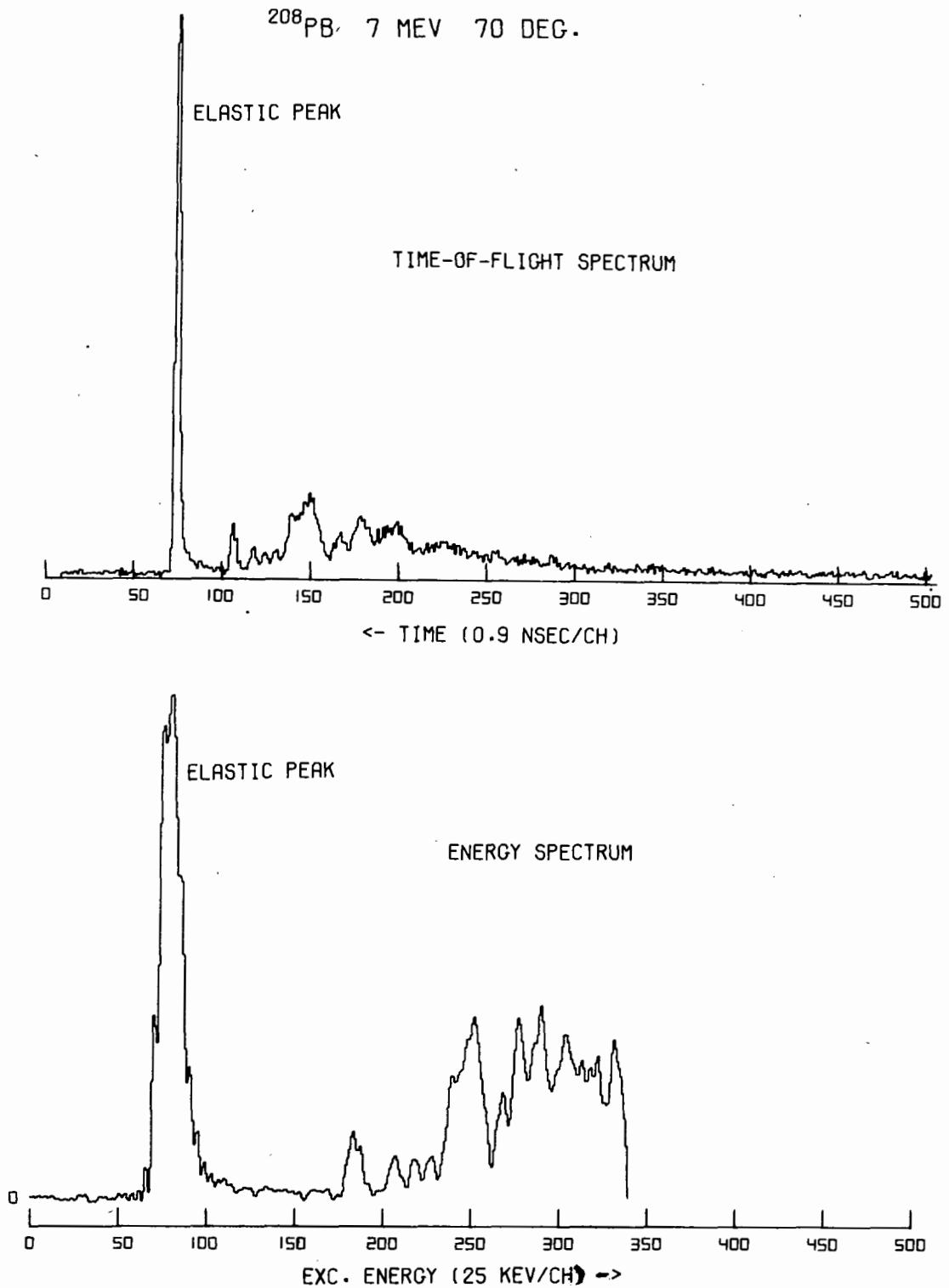


Fig. 1. A typical time-of-flight spectrum for ^{208}Pb with its transformed energy spectrum. The data were taken at an incident neutron energy of 7.00 MeV at an angle of 77.5 deg. with a 4 m flight path. The sample-out spectrum has not been subtracted from the time-of-flight spectrum. Note that the energy spectrum has been offset to allow negative excursions due to statistics in the subtraction of the sample-out.

completely stripped, the output information was written on magnetic tape for additional processing by a large computer.

Finite sample corrections were performed according to semianalytic recipes whose constants were obtained from fits to Monte Carlo results⁵. The corrections to the elastic differential cross sections were typically $\sim 18\%$ in the forward peak, 150 - 180% in the first minimum, and $\sim 16\%$ on the second maximum.

The final error analysis included uncertainties in the geometrical parameters (scatterer size, gas cell-to-scatterer distance, flight paths, etc.) and uncertainties in the finite sample corrections.

The measured differential elastic scattering cross sections were fitted by least squares to a Legendre series:

$$\sigma(\mu = \cos\theta) = \sum [(2k+1)/2] a_k P_k(\mu)$$

the points being weighted by the inverse of their variances which were computed by squaring the average of the upper and lower uncertainties. The common 7% uncertainty in absolute normalization was not included in the variances for the fitting. In order to prevent the fit from giving totally unrealistic values outside the angular range of our measurements, we resorted to the inelegant but workable process of adding three points equally spaced in angle between the largest angle of measurement and 175 degrees. The differential cross sections at the added points were chosen to approximate the diffraction pattern at large angles, but were assigned 50% errors.

RESULTS

Elastic Scattering Differential Cross Sections

Our elastic scattering differential cross sections for ^{208}Pb are shown in Figure 2 with Legendre fits to the data. Wick's Limit is shown and was used in the fitting. Complete elastic scattering angular distributions for ^{206}Pb and ^{207}Pb were not measured.

Our ^{208}Pb elastic scattering differential cross sections are compared at 7 MeV with the radiogenic lead data of Zafiratos *et al.*⁶ in Figure 3 where the two sets of data are seen to be in good agreement. ENDF/B III MAT 1136 angular distributions normalized to the integrals of our experimental data are also shown. They are in generally good agreement with the data.

Inelastic Scattering Differential Cross Sections

Our differential cross sections for inelastic scattering to the 2.615 MeV level in ^{208}Pb are shown in Figure 4 along with ENDF/B III MAT 1136 angular distributions. The angular distributions of neutrons scattered to this level become increasingly anisotropic as the incident neutron energy increases and direct interaction contributions become larger². We were unable to extract cross sections for inelastic scattering to this level at angles < 25 deg. and small-angle data are essential in fitting to a high order Legendre series required to describe highly irregular distributions. We therefore did not attempt to fit the data to obtain an angle-integrated cross section. The absolute values of the ENDF/B differential cross sections, per atom of ^{208}Pb , were used for the comparison. Our data at 5.50 and 8.50 MeV

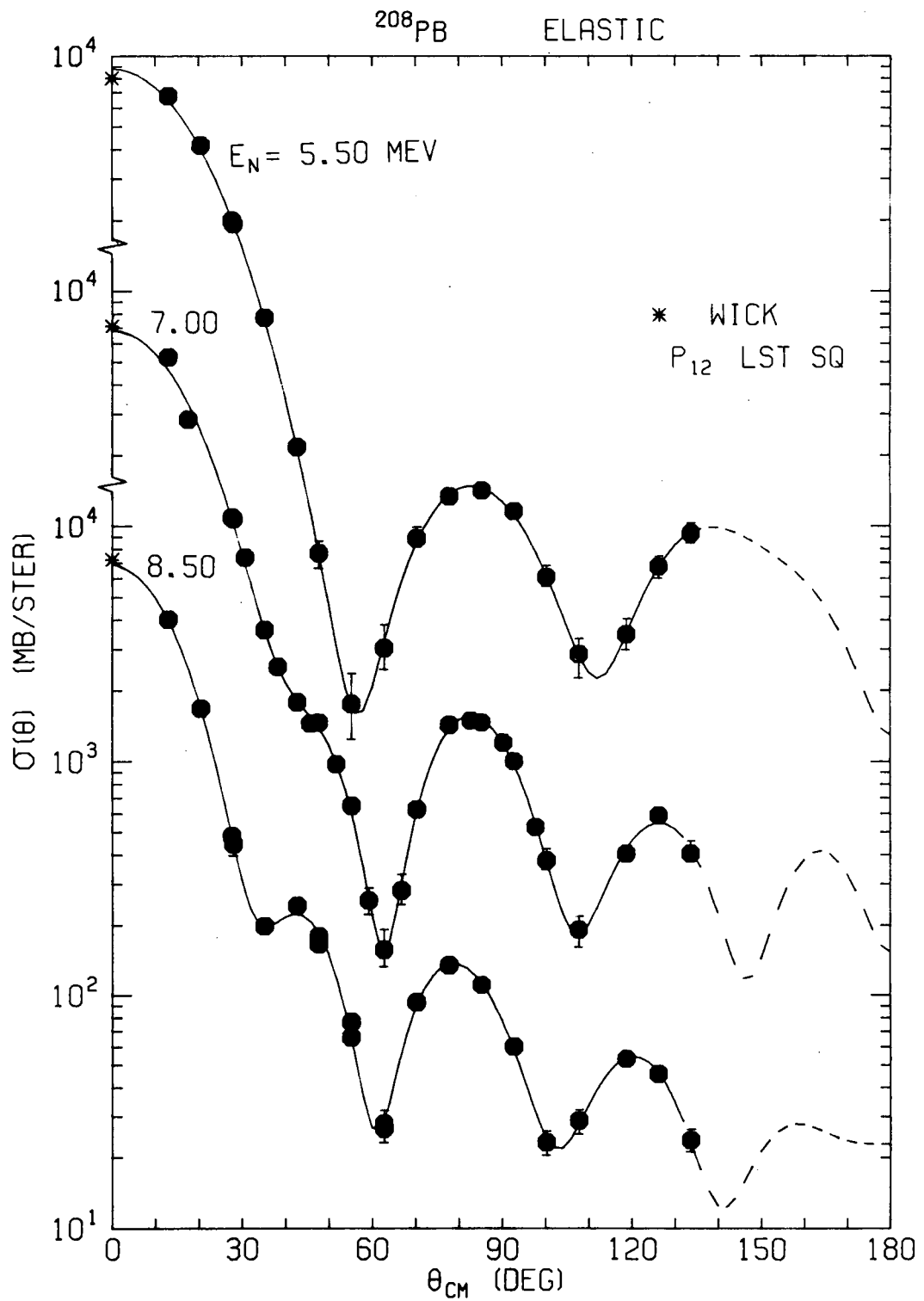


Fig. 2. Our ^{208}Pb neutron differential elastic center-of-mass cross sections with Legendre fits to the data. WICK indicates Wick's Limit which was used in the fitting. The 7% uncertainty in absolute normalization common to all points is not included in the error bars.

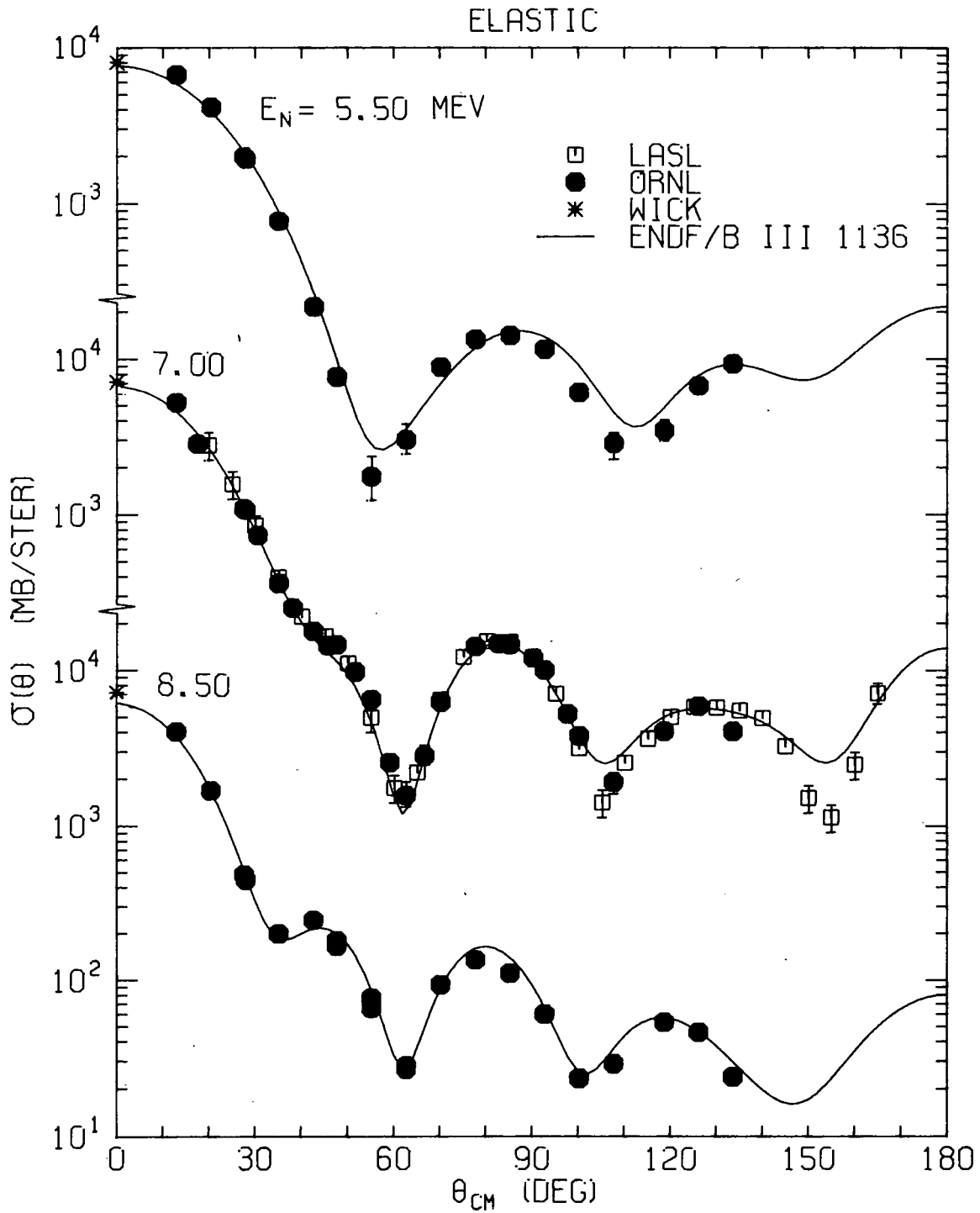


Fig. 3. Our ^{208}Pb neutron differential elastic center-of-mass cross sections compared with the data of Zafiratos *et al.*(LASL)⁶ and with the angular distributions of ENDF/B III MAT 1136. WICK indicates Wick's Limit.

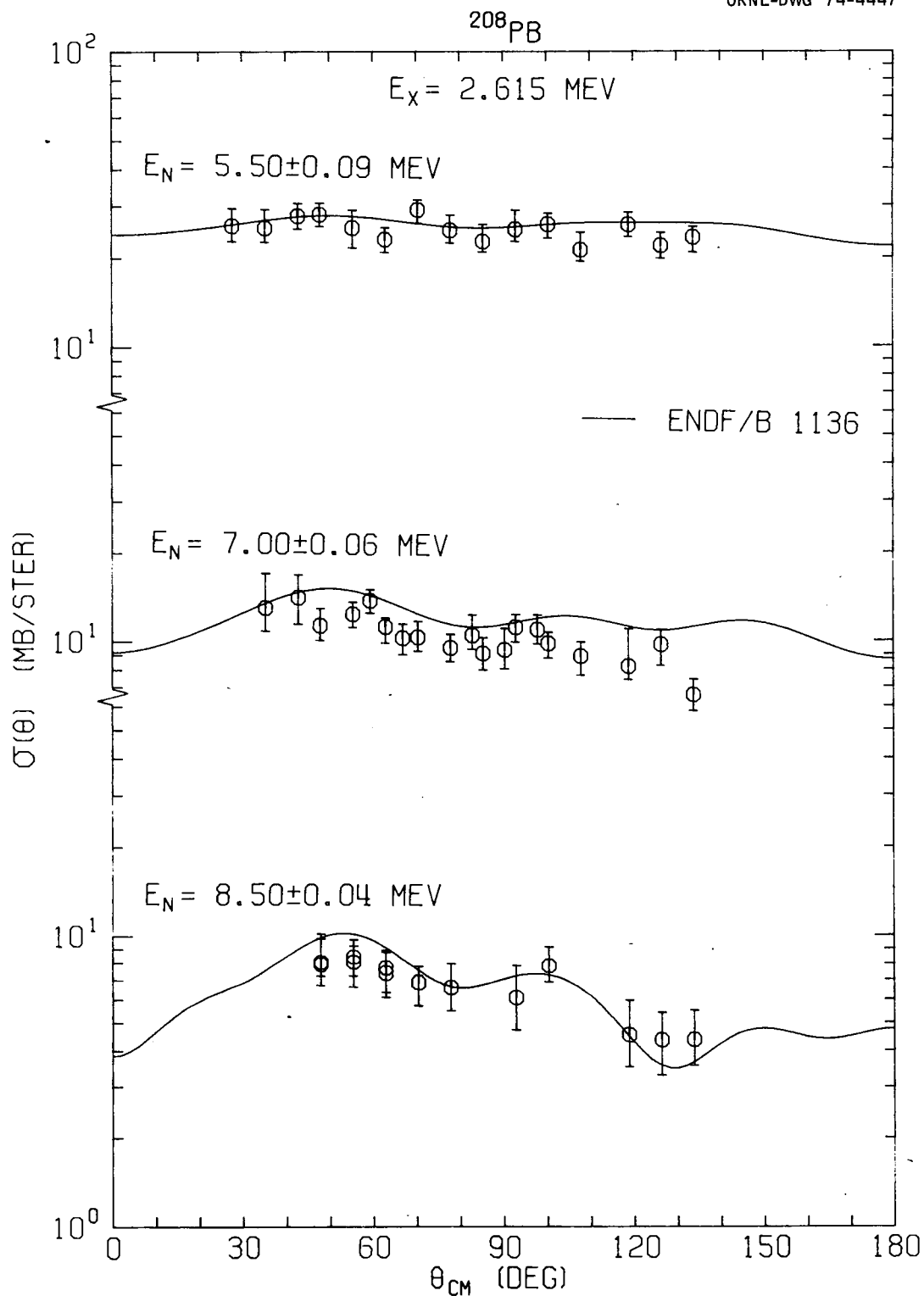


Fig. 4. Our differential center-of-mass cross sections for inelastic scattering to the 2.615 MeV level in ^{208}Pb compared with ENDF/B III MAT 1136 differential cross sections per atom of ^{208}Pb . The 7% uncertainty in absolute normalization common to all points is not included in our error bars.

agree with the ENDF/B III MAT 1136 differential cross section curves within experimental uncertainties but are systematically lower at 7.00 MeV.

Our differential cross sections for inelastic scattering to higher-lying levels or groups of levels in ^{208}Pb are shown in Figures 5 through 7. The angular distributions of neutrons scattered to these levels are isotropic within experimental uncertainties though some direct interaction contributions are known to be present in several of the groups of levels².

Excitation Functions

Our ^{208}Pb angle-integrated differential cross sections are shown as a function of incident neutron energy in Figures 8 through 10. The data of Towle and Gilboy⁷ and the curves from ENDF/B III MAT 1136 are also shown in Figure 8. The ENDF/B inelastic scattering cross sections are given per atom of ^{208}Pb .

The ENDF/B III MAT 1136 angle-integrated elastic scattering cross sections are obtained by subtracting the non-elastic from the total cross sections and agree with our data at 7 and 8.5 MeV but are lower than our data at 5.5 MeV by 14%.

The ENDF/B III MAT 1136 angle-integrated inelastic scattering cross sections were obtained by calculation² and the degree of agreement with experiment is gratifying. The calculations are generally higher than our data, at most by 80% for the 3.198 MeV level at 7 MeV. Direct interaction contributions were included in inelastic scattering to all the levels shown in Figure 8 except the 3.475 MeV level. Our data would indicate that there is some direct interaction contribution to inelastic scattering to this level also.

Figure 9 shows our angle-integrated cross sections as a function of incident neutron energy for inelastic scattering to groups of levels: 7 levels from 3.920 to 4.076 MeV, 12 levels from 4.125 to 4.480 MeV, and the sum of the inelastic scattering cross sections to these 19 levels from 3.920 to 4.480 MeV.

Above an excitation energy of 4.480 MeV the level spacing in ^{208}Pb is in the range of 10 - 20 keV therefore we could not resolve scattering to these levels. However some levels or groups of levels were preferentially excited at large enough energy intervals compared to our energy resolution so that extracting cross sections was feasible. Figure 10 shows our angle-integrated cross sections for inelastic scattering to groups of levels in the indicated excitation energy ranges.

Figures 11 and 12 show our angle-integrated cross sections for inelastic scattering to levels or groups of levels in ^{207}Pb as a function of incident neutron energy. Our data for ^{207}Pb were generally taken at just three angles except at 8.50 MeV where data were acquired at six angles. Our angle-integrated values were obtained by multiplying the average differential cross sections by 4π . The data of Cranberg *et al.*⁸ are also shown along with the curves from ENDF/B III MAT 1136. The data of Cranberg *et al.* were taken at an angle of 50 deg. and have been multiplied by 4π for the comparison. The ENDF/B III MAT 1136 cross sections are given per atom of ^{207}Pb .

The ENDF/B curves for ^{207}Pb are in generally good agreement with experimental data except for inelastic scattering to the levels of excitation energy from 3.057 to 3.298 MeV where our data lie above the ENDF/B curve.

Our angle-integrated cross sections for inelastic scattering to a group of levels in ^{206}Pb of excitation energy from 2.50 to 2.75 MeV are shown as a function of incident neutron energy

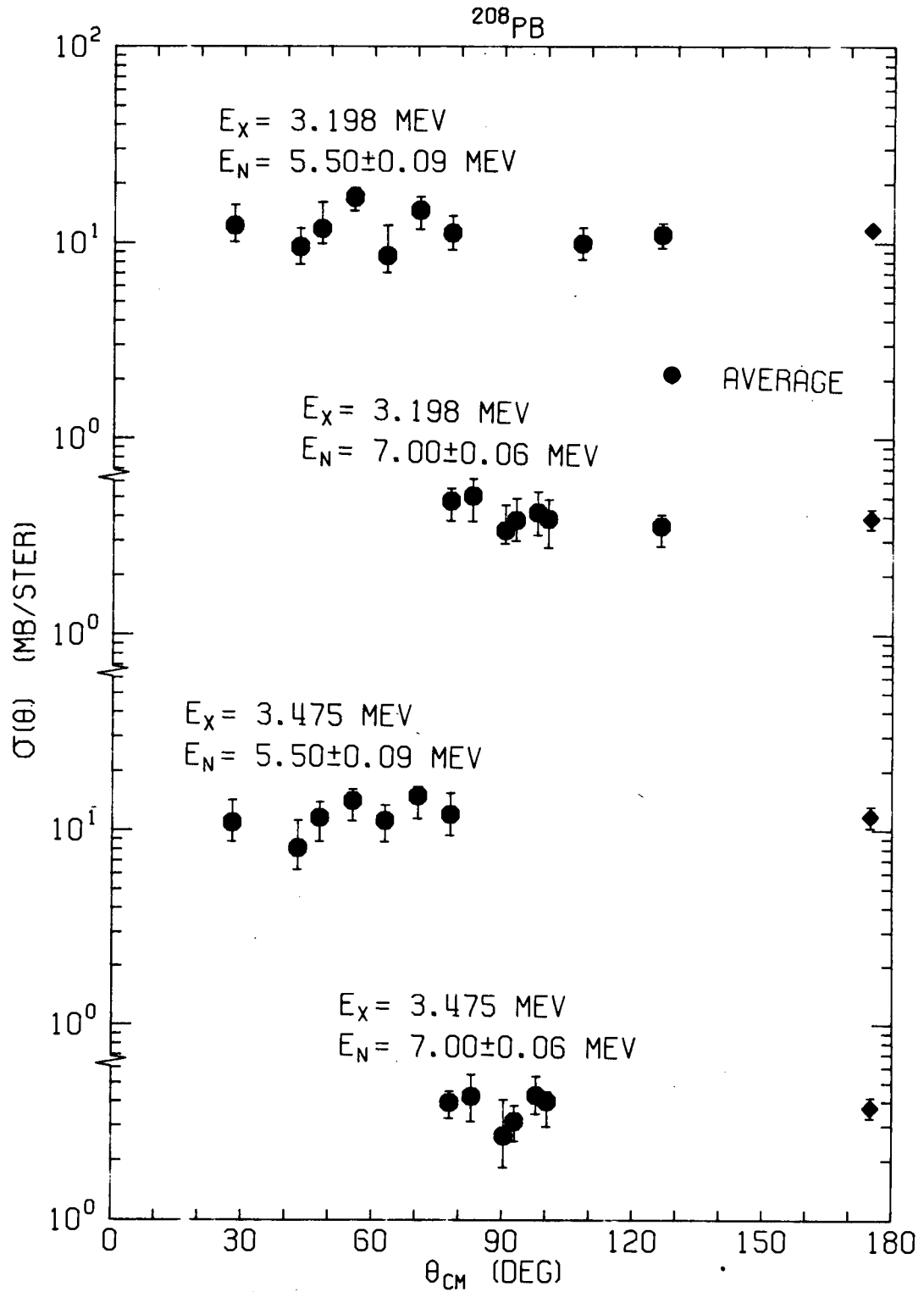


Fig. 5. Our differential center-of-mass cross sections for inelastic scattering to levels in ^{208}Pb . The 7% uncertainty in absolute normalization common to all points is not included in our error bars.

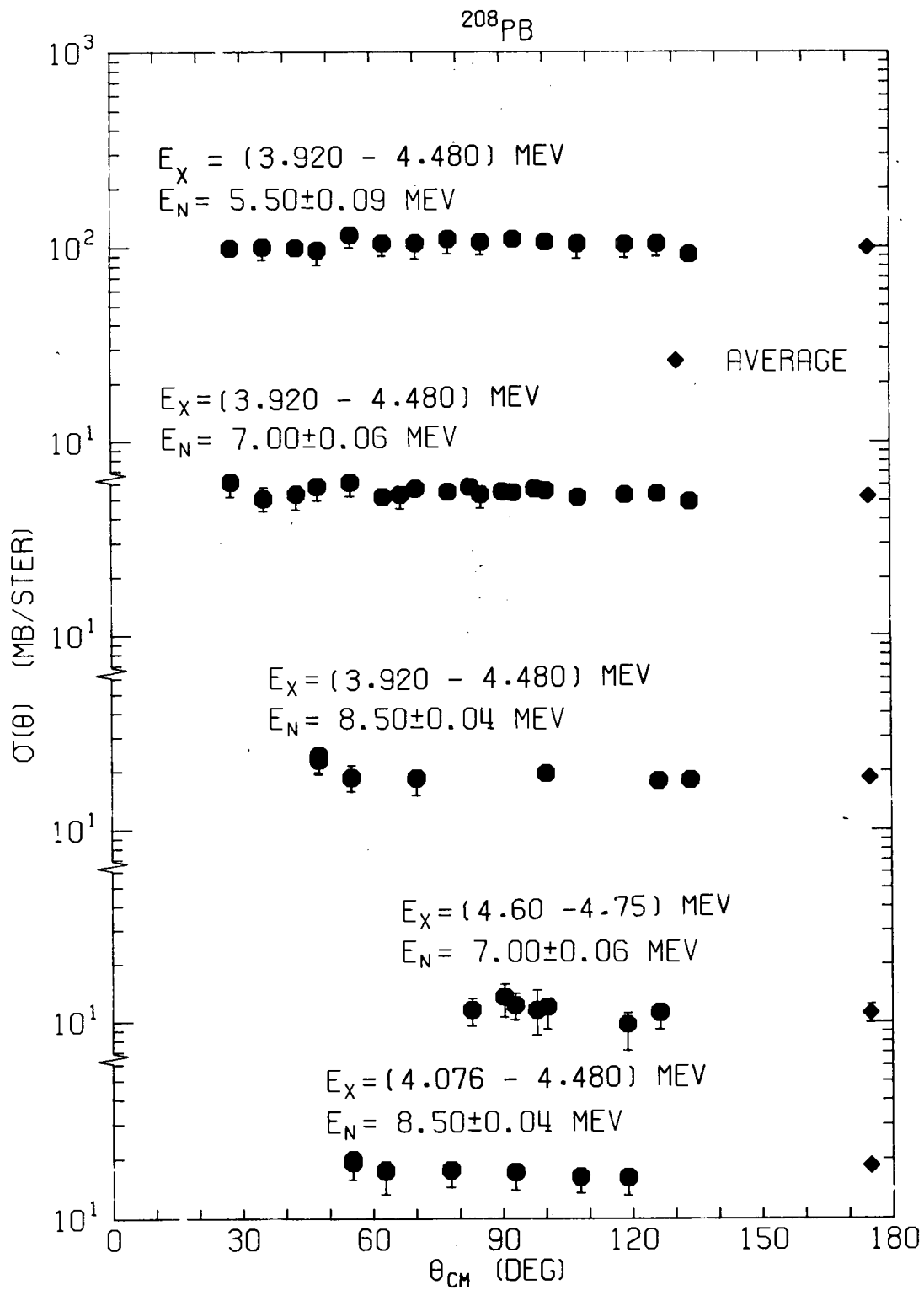


Fig. 6. Our differential center-of-mass cross sections for inelastic scattering to levels in ^{208}Pb . The 7% uncertainty in absolute normalization common to all points is not included in our error bars.

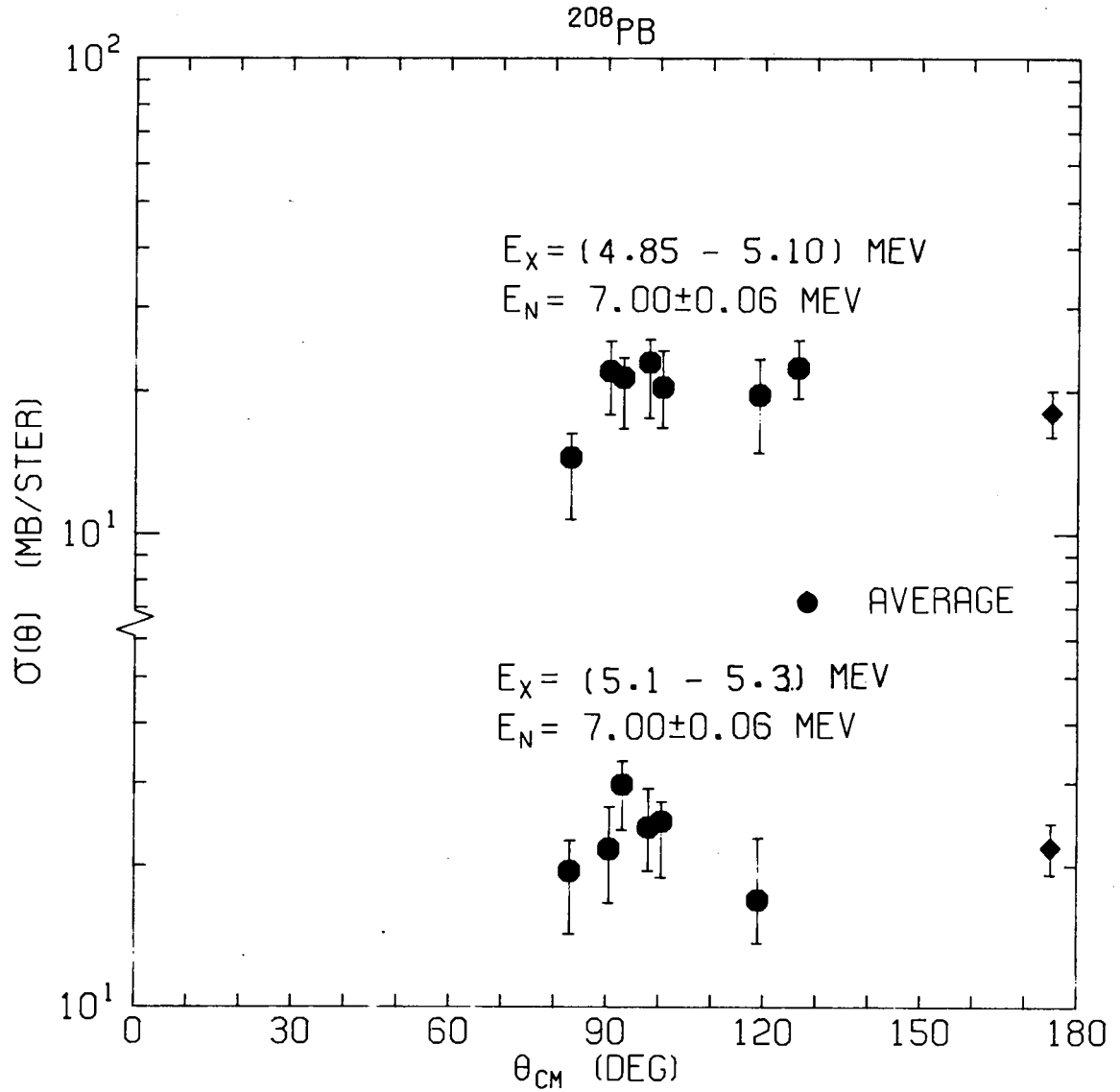


Fig. 7. Our differential center-of-mass cross sections for inelastic scattering to levels in ^{208}Pb . The 7% uncertainty in absolute normalization common to all points is not included in our error bars.

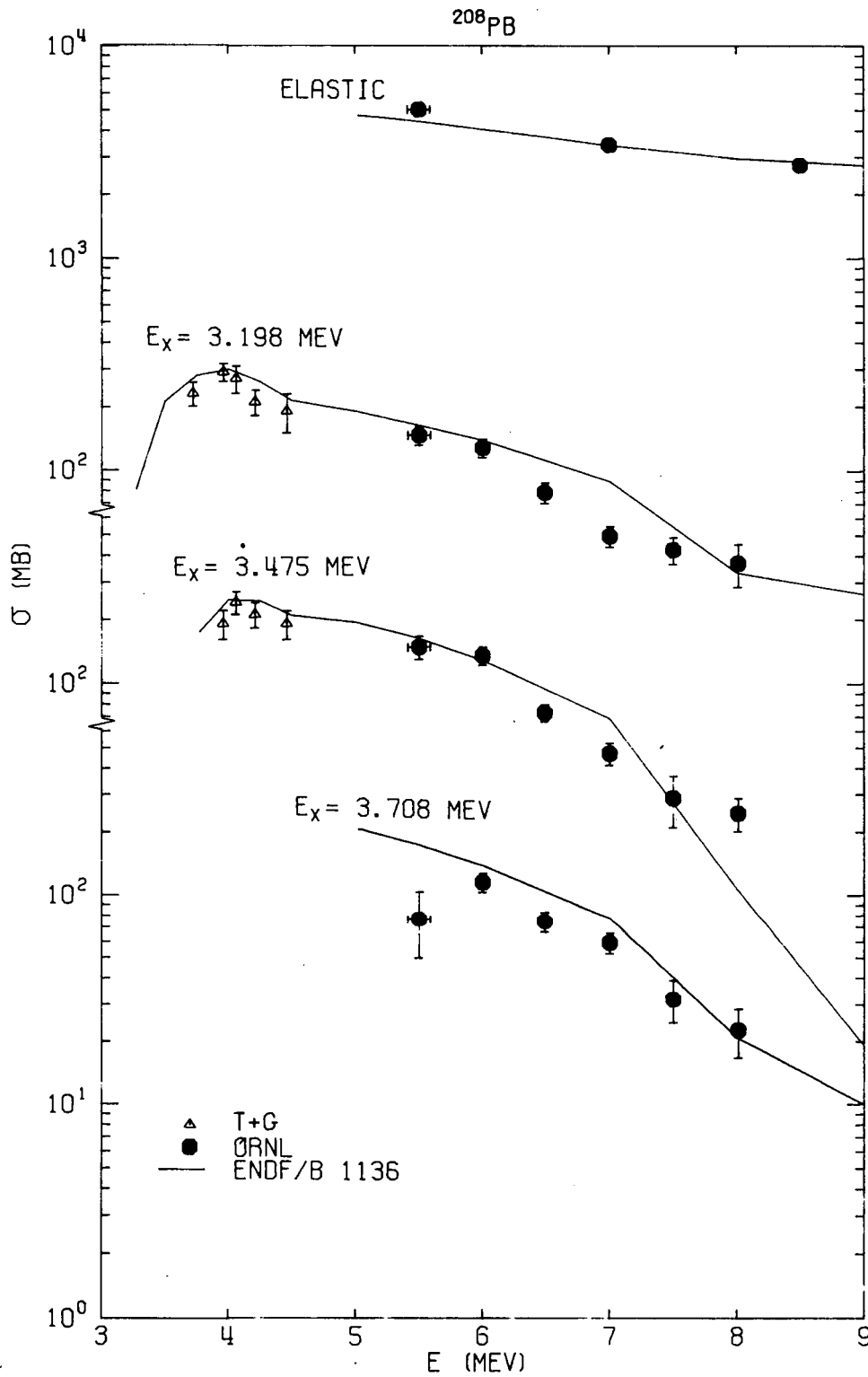


Fig. 8. Our angle-integrated neutron scattering cross sections for ^{208}Pb as a function of incident neutron energy. The data of Towle and Gilboy (T+G)⁷ and curves from ENDF/B III MAT 1136 per atom of ^{208}Pb are also shown. The 7% uncertainty in absolute normalization is included in our error bars.

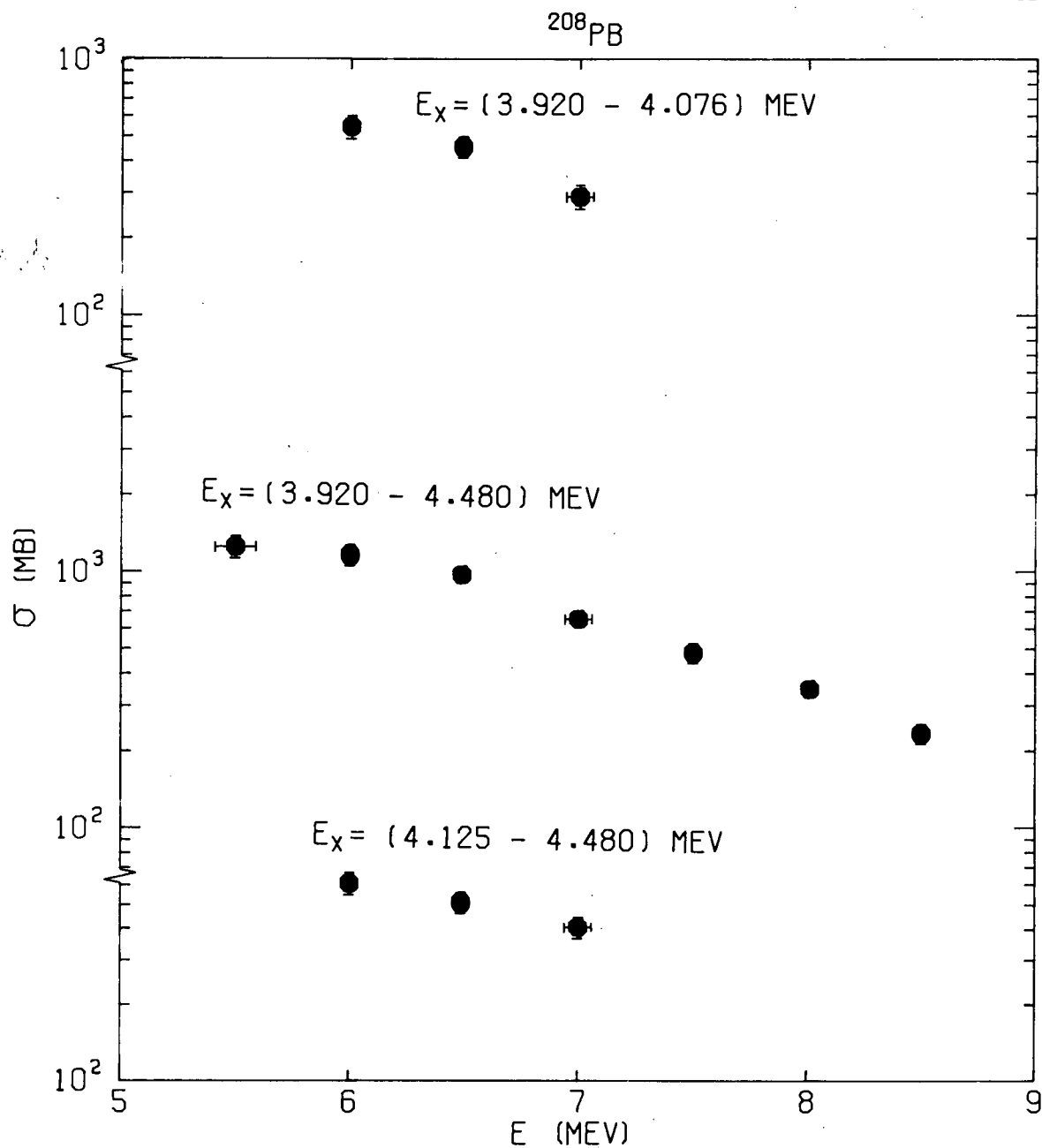


Fig. 9. Our angle-integrated neutron inelastic scattering cross sections to groups of levels in ^{208}Pb as a function of incident neutron energy. The 7% uncertainty in absolute normalization is included in our error bars.

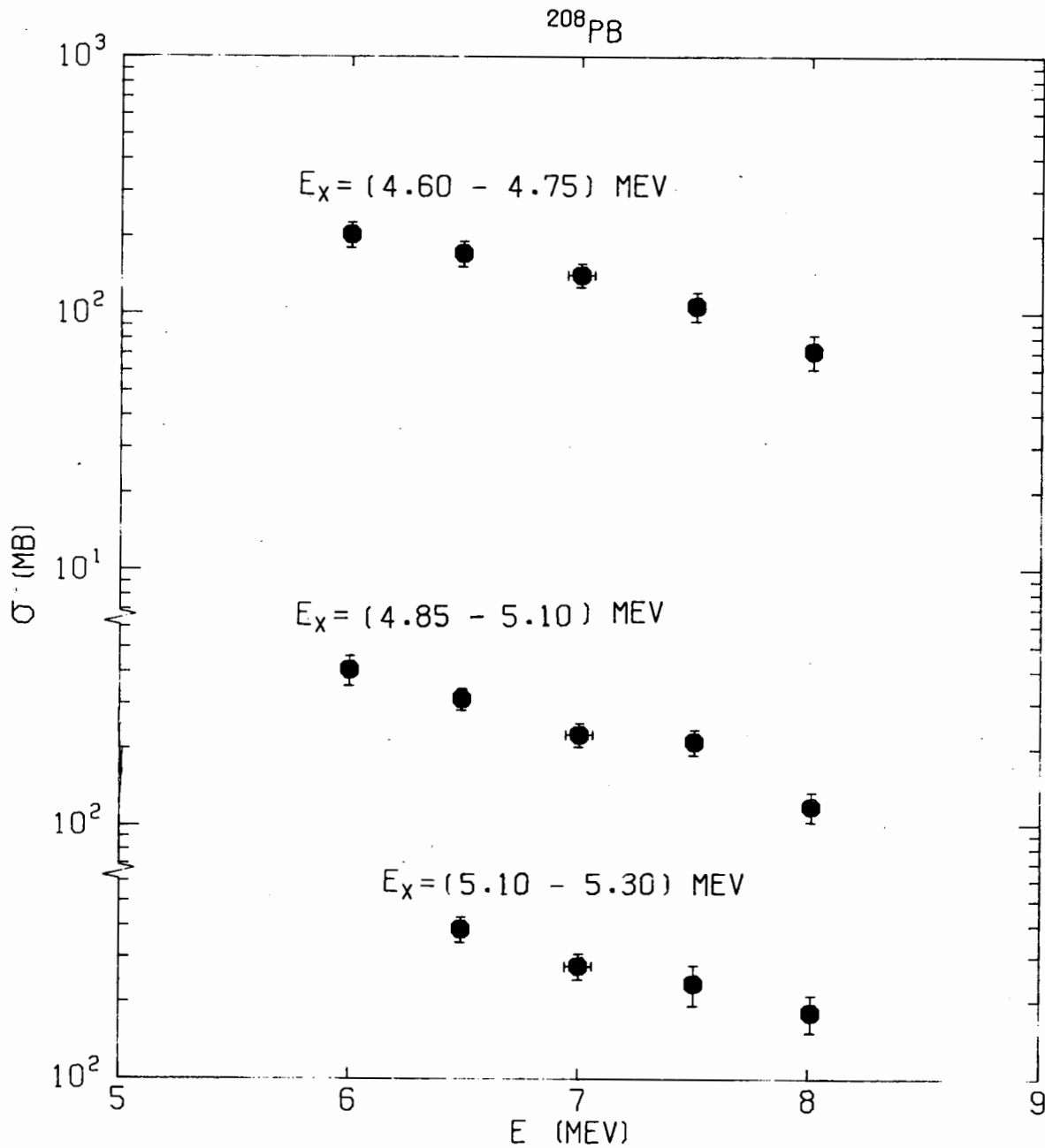


Fig. 10. Our angle-integrated neutron inelastic scattering cross sections to groups of levels in ^{208}Pb as a function of incident neutron energy. The 7% uncertainty in absolute normalization is included in our error bars.

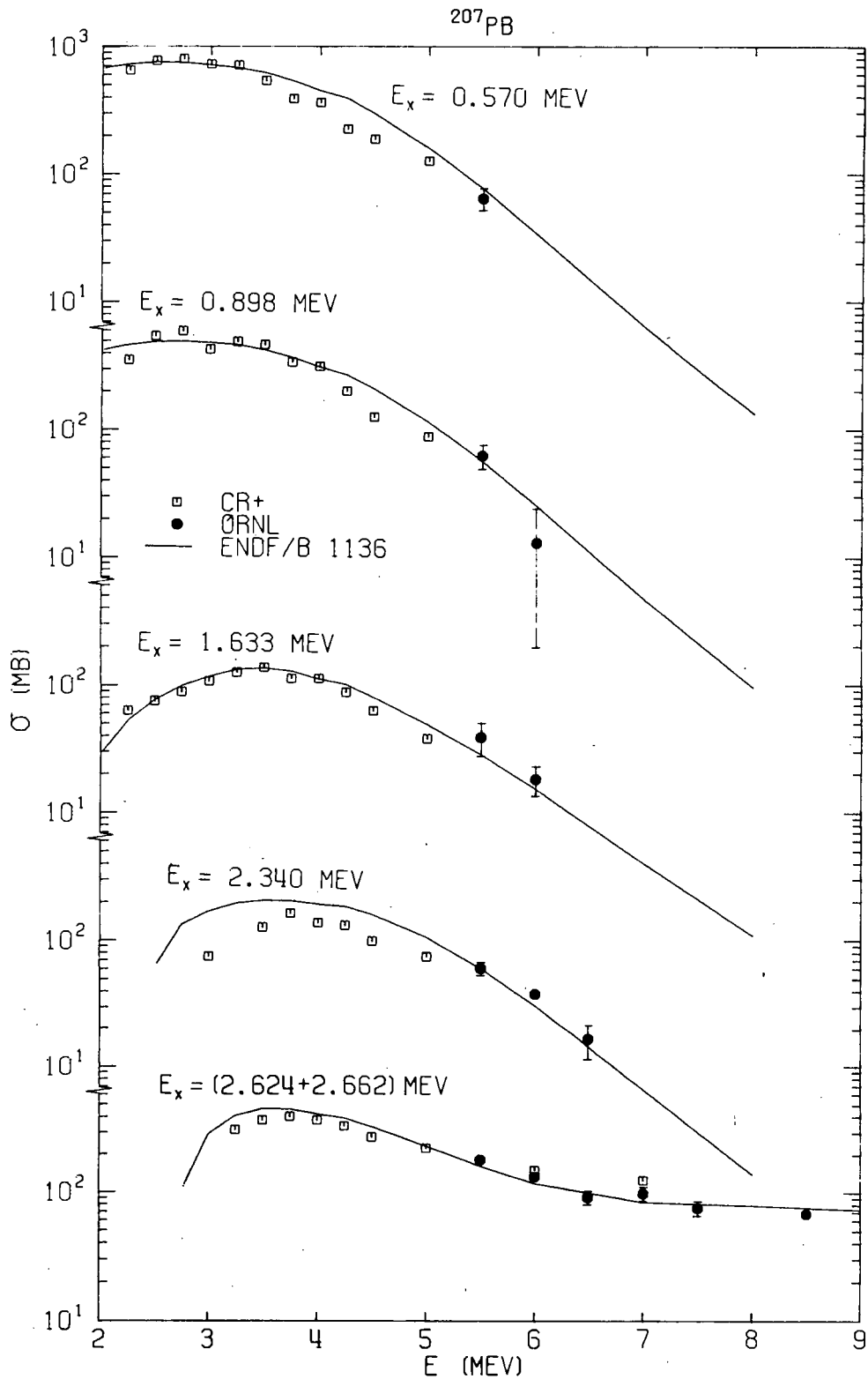


Fig. 11. Our angle-integrated neutron inelastic scattering cross sections to levels in ^{207}Pb as a function of incident neutron energy. The data of Cranberg *et al.* (CR+)⁸ and the curves from ENDF/B III MAT 1136 per atom of ^{207}Pb are also shown. The 7% uncertainty in absolute normalization is included in our error bars.

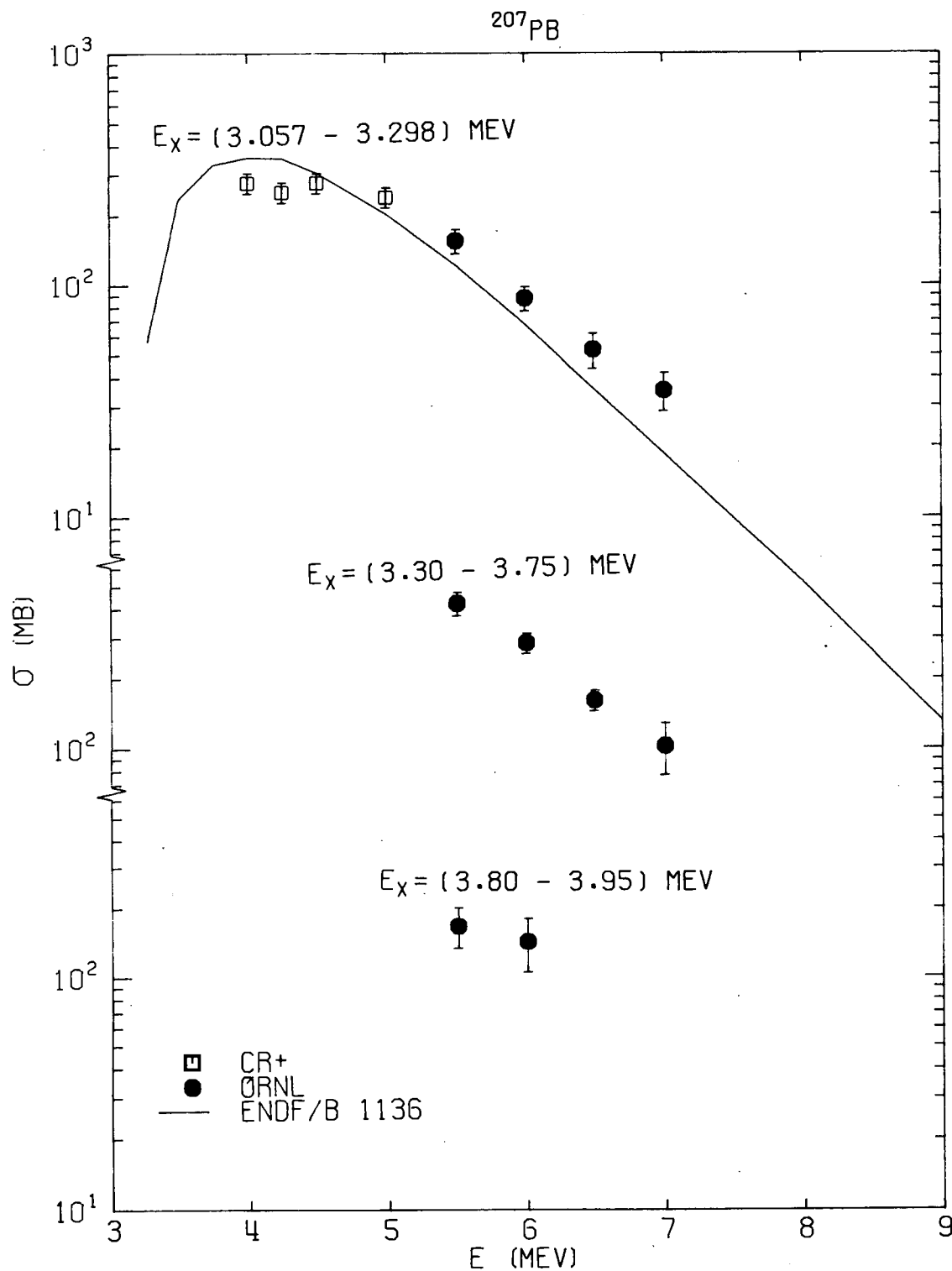


Fig. 12. Our angle-integrated neutron inelastic scattering cross sections to levels in ^{207}Pb as a function of incident neutron energy. The data of Cranberg *et al.* (CR+)⁸ and a curve from ENDF/B III MAT 1136 per atom of ^{207}Pb are also shown. The 7% uncertainty in absolute normalization is included in our error bars.

in Figure 13. Our data for ^{206}Pb were taken generally at three angles and our angle-integrated values were obtained by multiplying the average differential cross sections by 4π . The 50 deg. data of Cranberg *et al.*⁸ multiplied by 4π are also shown. The ENDF/B III MAT 1136 are for a group of 9 levels of excitation energy from 2.634 to 3.200 MeV and are given per atom of ^{206}Pb . The ENDF/B curve is in good agreement with experimental data from 5.5 to 8.5 MeV but is higher by roughly a factor of 2 at 3.5 MeV possibly due to the inclusion of more levels than measured by Cranberg *et al.*

Inelastic Scattering to the Continuum

Above an excitation energy of 3 MeV for ^{206}Pb and ^{207}Pb and an excitation energy of 5.3 MeV for ^{208}Pb inelastic scattering was treated as scattering to a continuum rather than attempting to resolve scattering to groups of levels or bands of excitation energy. Our angle-averaged cross sections for inelastic scattering to the continuum as a function of excitation energy are shown in Figures 14 through 16. Data are shown for ^{206}Pb below an excitation energy of 3 MeV in Figure 14 even though data below this energy were not used in the fitting which yielded nuclear temperatures. Preferential excitation of levels or groups of levels is evident in all the continuum cross sections.

The adequacy of an evaporation model in describing inelastic scattering to our "continua" may be judged from Figures 17 through 19 where $\text{SIG}(E \rightarrow E')/E'$ is plotted versus E' where $\text{SIG}(E \rightarrow E') =$ the angle-averaged cross section for scattering from incident neutron energy E to exit neutron energy dE' about E' . The straight lines are least squares fits to the logs of the data and yield the indicated temperatures. The uncertainties on the temperatures are fitting uncertainties only. An evaporation model is a better description of our continuum inelastic scattering cross sections at the higher incident neutron energies where groups of levels are less strongly excited. ENDF/B III MAT 1136 natural lead temperatures increase from a value of ~ 0.5 MeV at an incident neutron energy of 4.4 MeV to a value of ~ 0.85 MeV at an incident neutron energy of 8.5 MeV.

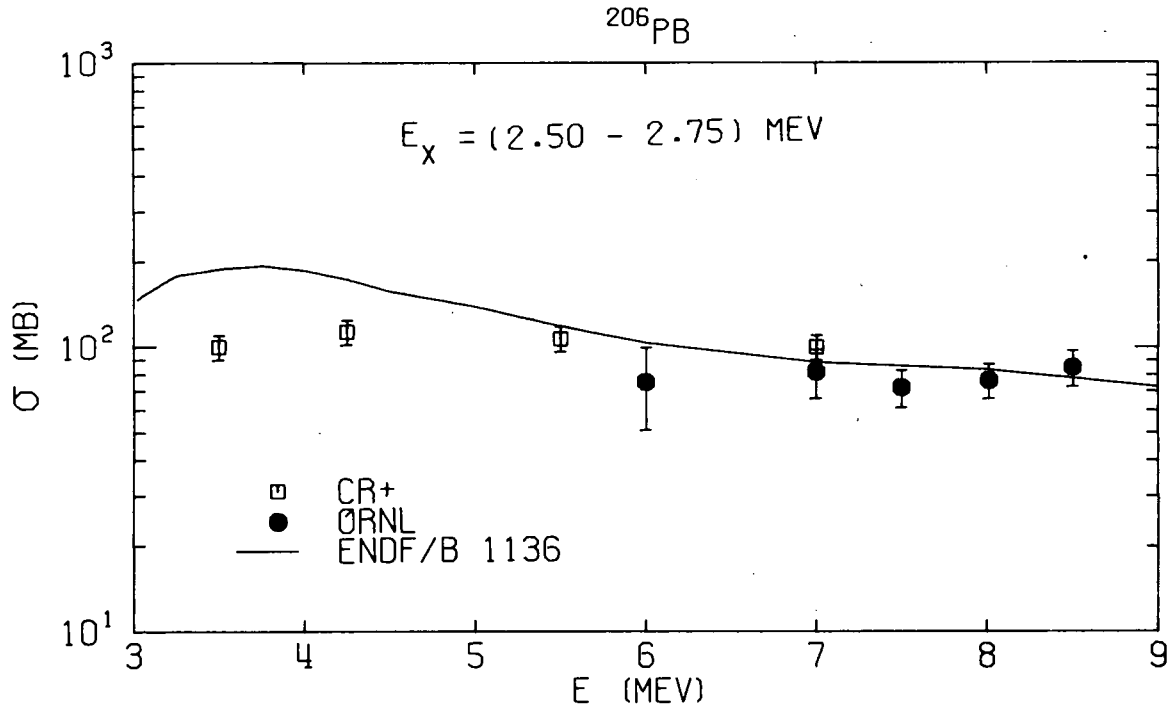


Fig. 13. Our angle-integrated cross sections for inelastic scattering to a group of levels in ^{206}Pb as a function of incident neutron energy. The data of Cranberg *et al.* (CR+)⁸ and a curve from ENDF/B III MAT 1136 per atom of ^{206}Pb are also shown. The 7% uncertainty in absolute normalization is included in our error bars.

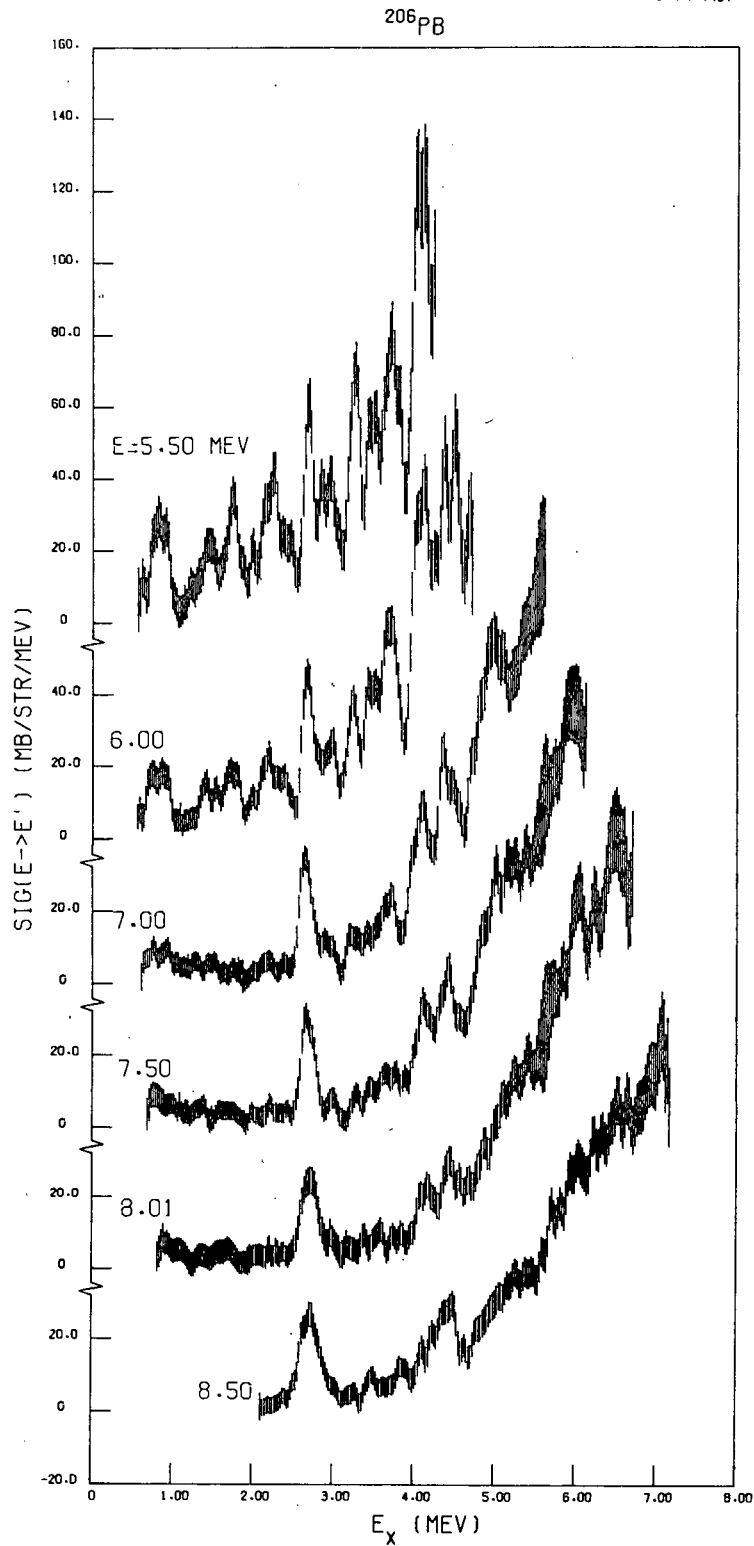


Fig. 14. Our angle-averaged double-differential cross sections for inelastic scattering to the "continuum" for ^{206}Pb as a function of excitation energy for incident neutron energies from 5.50 to 8.50 MeV.

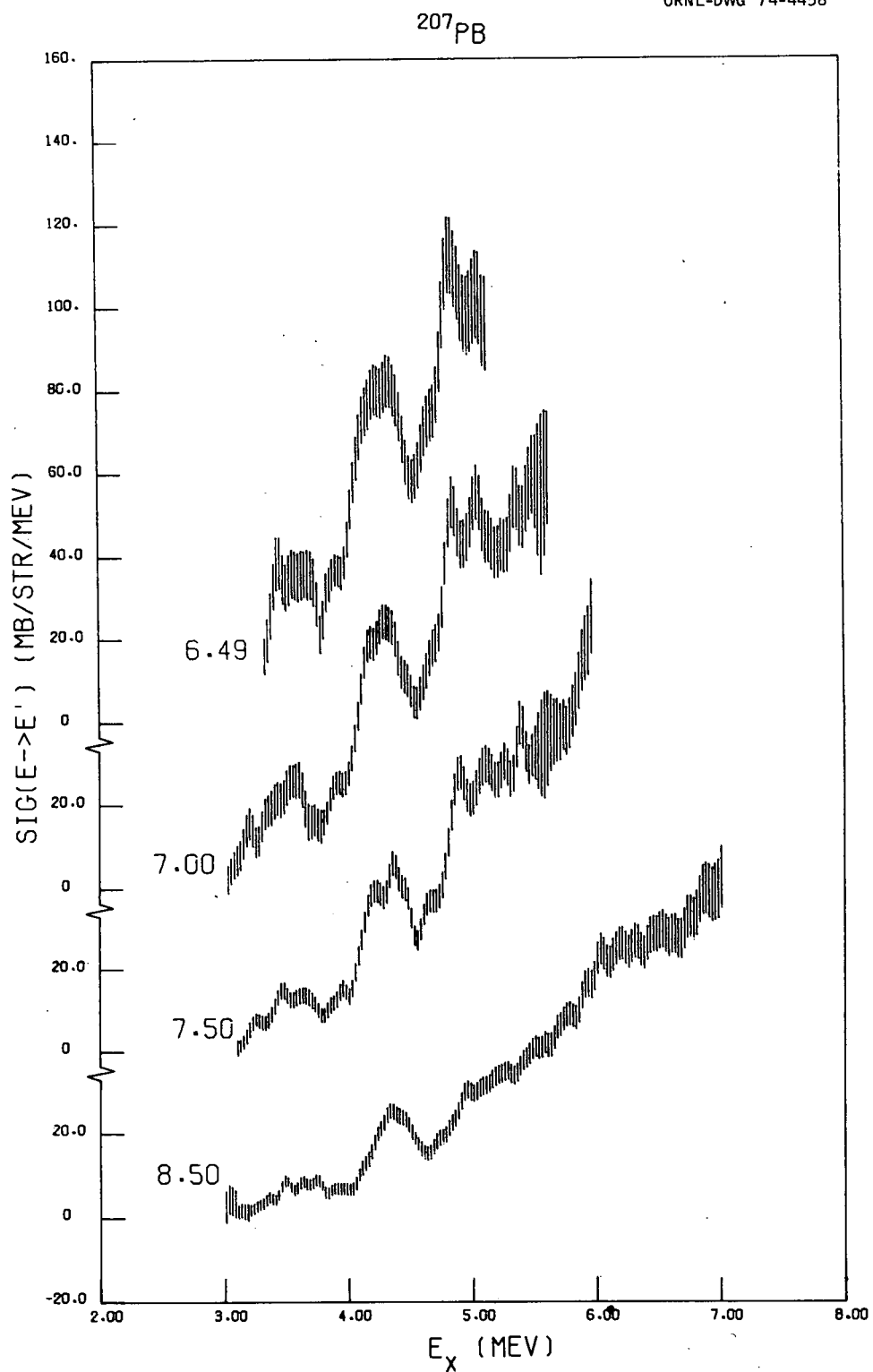


Fig. 15. Our angle-averaged double-differential cross sections for inelastic scattering to the "continuum" for ^{207}Pb as a function of excitation energy for incident neutron energies from 6.49 to 8.50 MeV.

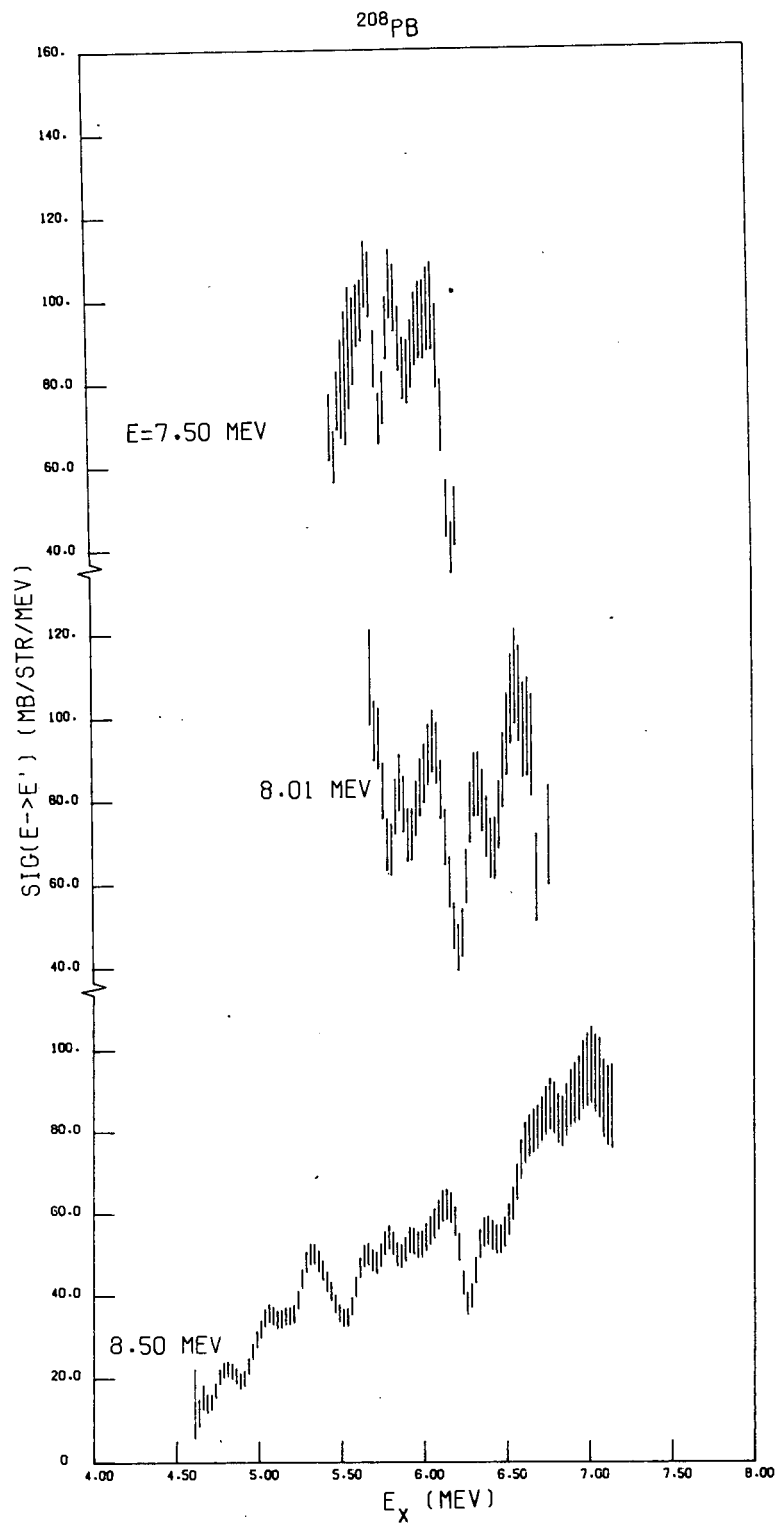


Fig. 16. Our angle-averaged double-differential cross sections for inelastic scattering to the "continuum" for ^{208}Pb as a function of excitation energy for incident neutron energies from 7.00 to 8.50 MeV.

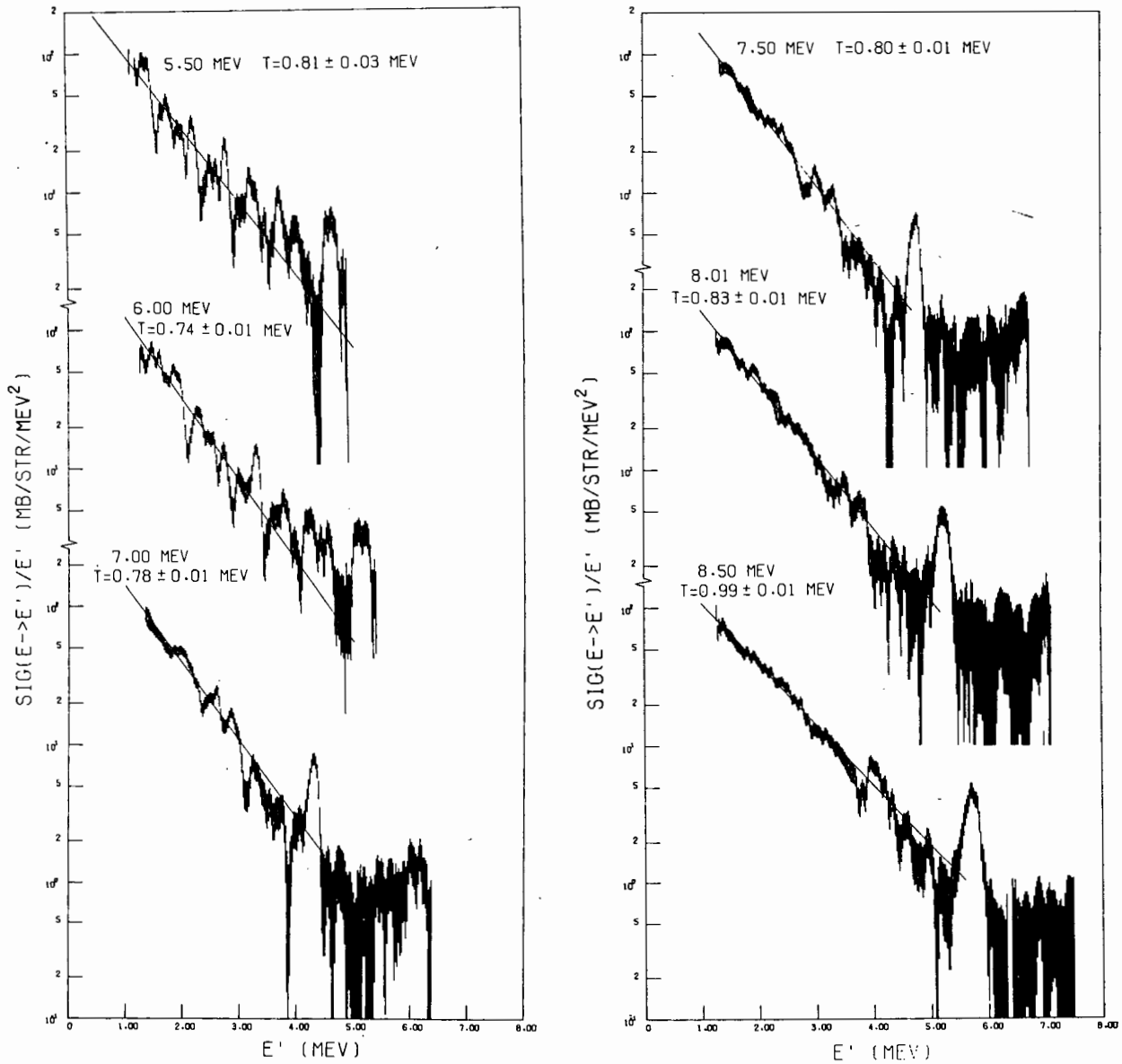


Fig. 17. ^{206}Pb angle-averaged cross sections for inelastic scattering to the continuum divided by the exit neutron energy, E' , for incident neutron energies from 5.50 to 8.50 MeV. The lines are least squares fits to the logs of the data with resulting temperatures, T , being indicated. The uncertainties on the temperatures are fitting uncertainties only. The fits were made over exit energies corresponding to excitation energies >3 MeV.

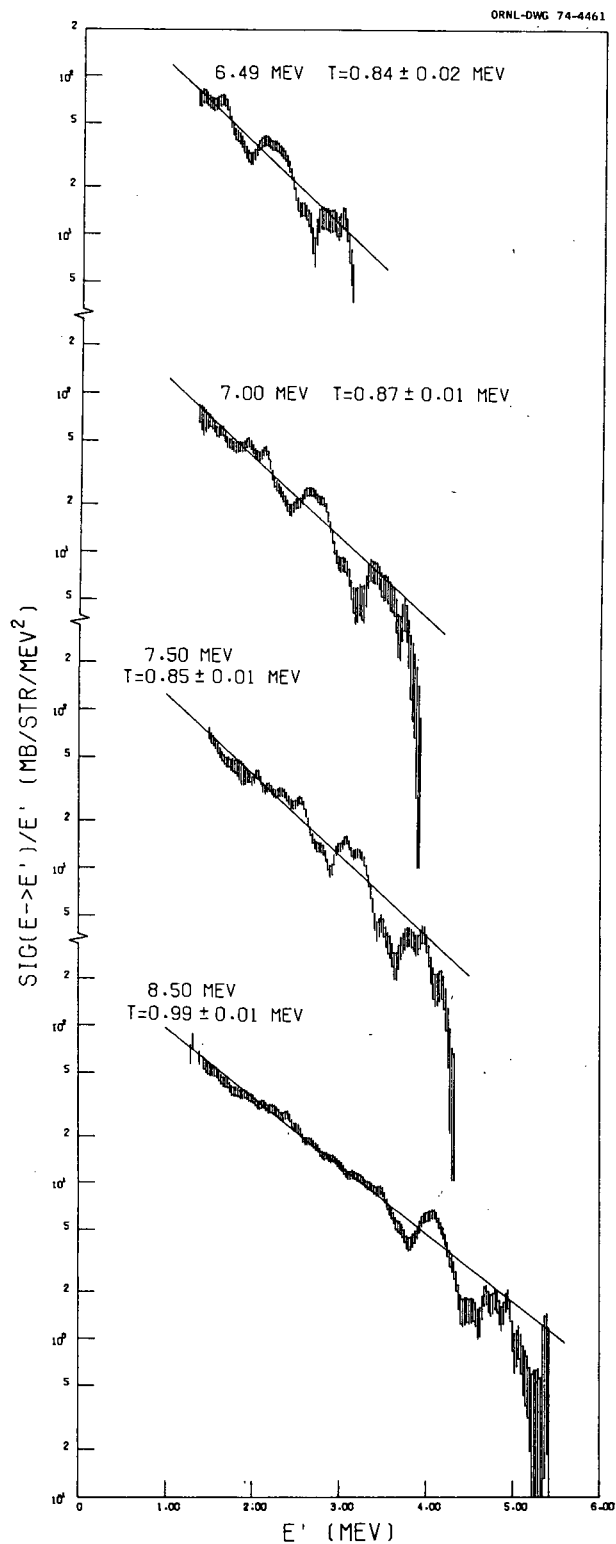


Fig. 18. ^{207}Pb angle-averaged cross sections for inelastic scattering to the continuum divided by the exit neutron energy, E' , for incident neutron energies from 6.49 to 8.50 MeV. The lines are least squares fits to the logs of the data with resulting temperatures, T , being indicated. The uncertainties on the temperatures are fitting uncertainties only. The fits were made over the entire range of exit energies.

ORNL-DWG 74-4462

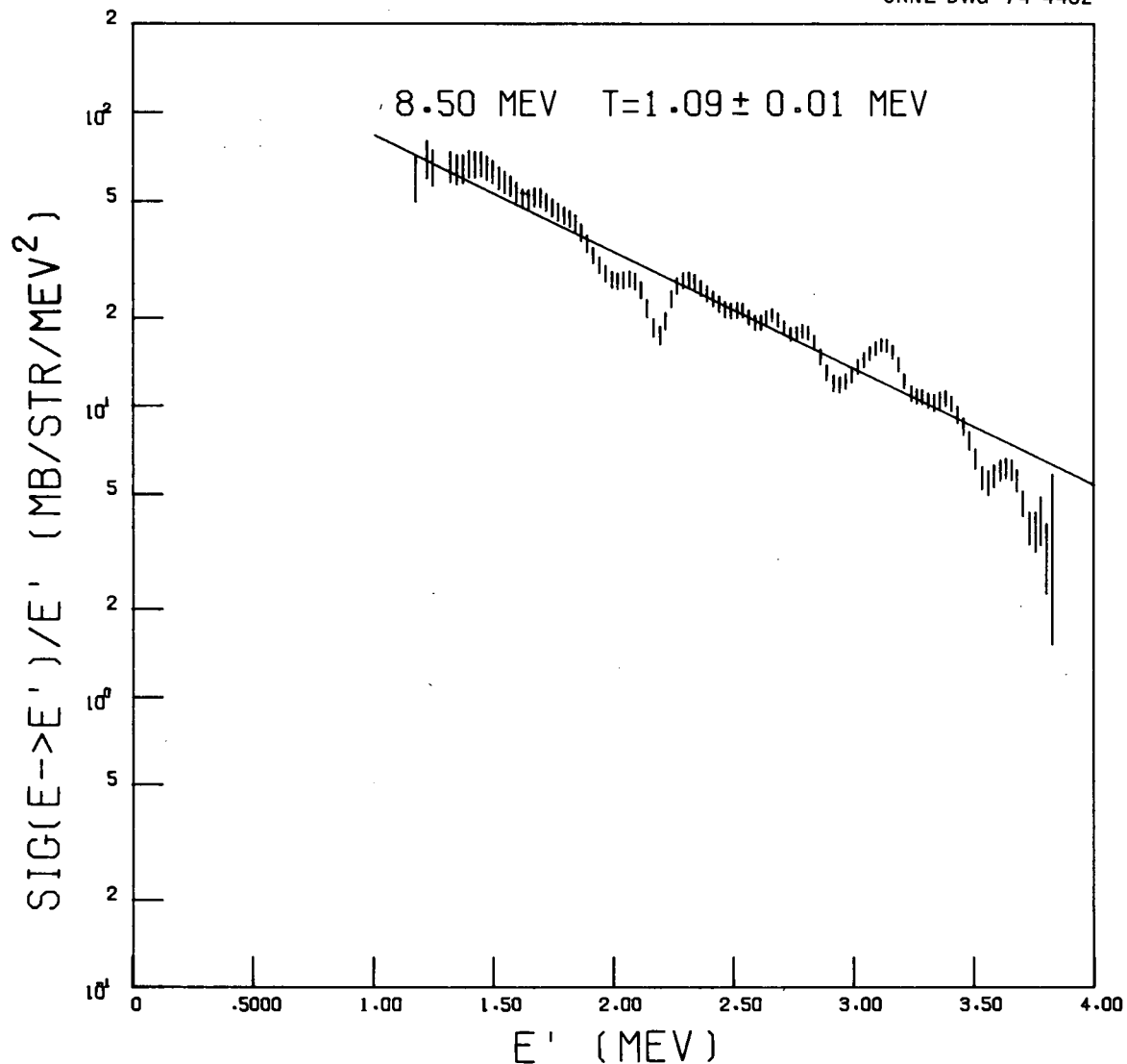


Fig. 19. ^{208}Pb angle-averaged cross sections for inelastic scattering to the continuum divided by the exit neutron energy, E' , for incident neutron energies from 7.00 to 8.50 MeV. The line is a least squares fit to the logs of the 8.50 MeV data with the resulting temperature, T , being indicated. The uncertainty on the temperature is a fitting uncertainty only. The fit was made over the entire range of exit energy.

CONCLUSIONS

Our data are in general agreement with the results of others. ENDF/B III MAT 1136 neutron elastic and inelastic scattering cross sections are generally in good agreement with experimental data from 3.5 to 8.5 MeV.

ACKNOWLEDGMENTS

Many have contributed to this experimental program at one time or another and we would like to thank them for their contributions. In particular, we would like to acknowledge the help of J. K. Dickens, J. W. McConnell, J. A. Biggerstaff, A. M. Marusak, P. H. Stelson, C. O. LeRigoleur, and E. Hungerford.

We are deeply indebted to F. C. Maienschein, director of the Neutron Physics Division, for his support of the experiment with the use of computers in report preparation and type setting which produced this report and the other six of our last seven reports.

REFERENCES

1. F. G. Perey and W. E. Kinney, "Carbon Neutron Elastic- and Inelastic-Scattering Cross Sections from 4.5 to 8.5 MeV", ORNL-4441 (December 1970).

F. G. Perey, C. O. LeRigoleur and W. E. Kinney, "Nickel-60 Neutron Elastic- and Inelastic-Scattering Cross Sections from 6.5 to 8.5 MeV", ORNL-4523 (April 1970).

W. E. Kinney and F. G. Perey, "Neutron Elastic- and Inelastic-Scattering Cross Sections from ^{56}Fe in the Energy Range 4.19 to 8.56 MeV", ORNL-4515 (June 1970).

F. G. Perey and W. E. Kinney, "Calcium Neutron Elastic- and Inelastic-Scattering Cross Sections from 4.0 to 8.5 MeV", ORNL-4519 (April 1970).

F. G. Perey and W. E. Kinney, "Sulfur Neutron Elastic- and Inelastic-Scattering Cross Sections from 4 to 8.5 MeV", ORNL-4539 (June 1970).

W. E. Kinney and F. G. Perey, "Neutron Elastic- and Inelastic- Scattering Cross Sections for Co in the Energy Range 4.19 to 8.56 MeV", ORNL-4549 (June 1970).

W. E. Kinney and F. G. Perey, "Neutron Elastic- and Inelastic- Scattering Cross Sections for Mg in the Energy Range 4.19 to 8.56 MeV", ORNL-4550 (June 1970).

W. E. Kinney and F. G. Perey, "Neutron Elastic- and Inelastic- Scattering Cross Sections for Si in the Energy Range 4.19 to 8.56 MeV", ORNL-4517 (July 1970).

F. G. Perey and W. E. Kinney, "Neutron Elastic and Inelastic- Scattering Cross Sections for Na in the Energy Range of 5.4 to 8.5 MeV", ORNL-4518 (August 1970).

W. E. Kinney and F. G. Perey, "Al Neutron Elastic- and Inelastic- Scattering Cross Sections from 4.19 to 8.56 MeV", ORNL-4516 (October 1970).

F. G. Perey and W. E. Kinney, "V Neutron Elastic- and Inelastic- Scattering Cross Sections from 4.19 to 8.56 MeV", ORNL-4551 (October 1970).

F. G. Perey and W. E. Kinney, "Neutron Elastic- and Inelastic- Scattering Cross Sections for Yttrium in the Energy Range 4.19 to 8.56 MeV", ORNL-4552 (December 1970).

W. E. Kinney and F. G. Perey, "Neutron Elastic- and Inelastic- Scattering Cross Sections for Oxygen in the Energy Range 4.34 to 8.56 MeV", ORNL-4780 (April 1972).

W. E. Kinney and F. G. Perey, "W Neutron Elastic- and Inelastic- Scattering Cross Sections from 4.34 to 8.56 MeV", ORNL-4803 (May 1973).

W. E. Kinney and F. G. Perey, " ^{238}U Neutron Elastic-Scattering Cross Sections from 6.44 to 8.56 MeV", ORNL-4804 (June 1973).

W. E. Kinney and F. G. Perey, "Natural Titanium Neutron Elastic and Inelastic Scattering Cross Sections from 4.07 to 8.56 MeV", ORNL-4810 (October 1973).

W. E. Kinney and F. G. Perey, "Natural Nickel and ^{60}Ni Neutron Elastic and Inelastic Scattering Cross Sections from 4.07 to 8.56 MeV", ORNL-4807 (January 1974).

- W. E. Kinney and F. G. Perey, "Natural Chromium and ^{52}Cr Neutron Elastic and Inelastic Scattering Cross Sections from 4.07 to 8.56 MeV", ORNL-4806 (January 1974).
- F. G. Perey and W. E. Kinney, "Nitrogen Neutron Elastic and Inelastic Scattering Cross Sections from 4.34 to 8.56 MeV", ORNL-4805 (February 1974).
- W. E. Kinney and F. G. Perey, " ^{54}Fe Neutron Elastic and Inelastic Scattering Cross Sections from 4.34 to 8.56 MeV", ORNL-4907 (February 1974).
- W. E. Kinney and F. G. Perey, " ^{63}Cu and ^{65}Cu Neutron Elastic and Inelastic Scattering Cross Sections from 5.50 to 8.50 MeV", ORNL-4908 (February 1974).
2. C. Y. Fu and F. G. Perey, "An Evaluation of Neutron and Gamma-Ray-Production Cross Sections for Lead", ORNL-4765 (March 1972).
 3. W. E. Kinney, "Neutron Elastic and Inelastic Scattering from ^{56}Fe from 4.60 to 7.55 MeV", ORNL-TM-2052, (January 1968).
 4. R. E. Textor and V. V. Verbinski, "05S: A Monte Carlo Code for Calculating Pulse Height Distributions Due to Monoenergetic Neutrons Incident on Organic Scintillators", ORNL-4160 (February 1968).
 5. W. E. Kinney, Nucl. Instr. and Methods 83, 15 (1970).
 6. C. D. Zafiratos, T. A. Oliphant, J. S. Levin, and L. Cranberg, Phys. Rev. Letters 14, 913 (1965).
 7. J. H. Towle and W. B. Gilboy, Nucl. Phys. 44, 256 (1963).
 8. Lawrence Cranberg, Thomas A. Oliphant, Jules Levin, and C. D. Zafiratos, Phys. Rev. 159, 969 (1967).

APPENDIX

Tabulated Values of ^{208}Pb
Neutron Elastic Scattering Cross Sections
and
Cross Sections for Inelastic Scattering
to Discrete Levels in ^{206}Pb , ^{207}Pb , and ^{208}Pb

Our measured values for ^{208}Pb neutron elastic scattering cross sections and cross sections for inelastic scattering to discrete levels in ^{206}Pb , ^{207}Pb , and ^{208}Pb are tabulated below. The uncertainties in differential cross sections, indicated by Δ in the tables, are relative and do *not* include a $\pm 7\%$ uncertainty in detector efficiency which is common to all points. The $\pm 7\%$ uncertainty is included in the integrated and average values. The total cross sections, σ_T , are those we used in the computation of Wick's Limit and were not measured by us.

We have not included the cross sections for inelastic scattering to the continuum. They are available from the National Neutron Cross Section Center, Brookhaven National Laboratory, or from us.

^{208}Pb cross sections may be found on pages 29 through 39, ^{207}Pb cross sections on pages 40 through 44, and ^{206}Pb cross sections on page 45.

Inelastic scattering to the sums of discrete levels indicated in the tables would more properly be described as scattering to bands of excitation energy because of the large number of levels in the Pb isotopes. The correspondence is given in the following table.

Discrete Levels, MeV	Excitation Energy, MeV	Discrete Levels, MeV	Excitation Energy, MeV	Discrete Levels, MeV	Excitation Energy MeV
^{208}Pb		^{207}Pb		^{206}Pb	
3.961 + 4.076	3.92–4.076	3.202 + 3.222	3.057–3.298	2.634	2.634–3.200
4.076 + 4.323	4.076–4.480	3.450	3.30–3.50		
4.323	4.125–4.480	3.450 + 3.600	3.30–3.75		
4.698	4.60–4.75	3.776	3.75–3.95		
4.974 + 5.038	4.85–5.10	4.128 + 4.368 + 4.386	4.00–4.45		
5.254	5.1–5.3				

Energy resolutions for ^{207}Pb and ^{206}Pb are the same as those for ^{208}Pb , not zero as shown in the tables.

²⁰⁸Pb CROSS SECTIONS

$E_n = 5.50 \pm 0.09$ MeV
Elastic Scattering

θ_{cm} deg.	$d\sigma/d\omega$ mb/str	Δ (%)	
		+	-
13.00	6745.71	4.9	4.3
20.50	4168.53	5.1	5.2
27.62	1998.09	5.6	5.4
28.00	1930.70	5.4	7.9
35.15	773.96	5.8	5.3
42.69	217.13	8.0	7.4
47.71	76.99	12.4	13.7
55.23	17.56	34.7	29.3
62.75	30.35	25.6	19.1
70.26	88.89	11.7	7.8
77.77	134.07	8.8	7.2
85.28	142.03	9.2	7.4
92.78	115.90	10.0	7.4
100.27	60.97	11.7	8.7
107.77	28.61	16.5	21.0
118.74	34.72	16.6	14.2
126.22	67.40	10.7	10.7
133.71	93.35	10.4	9.3

$\int(d\sigma/d\omega)d\omega = 4995.68 \text{ mb} \pm 7.3 \%$
Wick's Limit = $8065.10 \text{ mb} \pm 7.3 \%$
 $\sigma_T = 6.96 \text{ b} \pm 1.0 \%$

Legendre Fit, Order = 12

k	a_k	Δ (%)
0	795.08911	2.2
1	606.93506	2.6
2	521.60181	2.7
3	424.97607	2.9
4	329.31567	3.1
5	231.55000	3.9
6	125.58133	6.0
7	71.27576	9.5
8	42.31218	11.9
9	19.07111	20.8
10	6.00756	52.3
11	1.34368	147.5
12	-0.56086	328.5

$E_n = 5.50 \pm 0.09$ MeV
(n,n') to: 2.615 MeV Level

θ_{cm} deg.	$d\sigma/d\omega$ mb/str	Δ (%)	
		+	-
27.68	25.73	14.8	11.3
35.22	25.29	15.8	10.2
42.76	27.74	10.7	9.2
47.78	28.05	9.7	8.6
55.32	25.32	14.8	14.4
62.84	23.10	9.7	9.6
70.36	29.04	8.5	9.6
77.87	24.77	12.7	9.2
85.38	22.70	14.3	7.8
92.88	24.91	16.3	8.8
100.37	25.89	9.0	10.0
107.87	21.22	15.0	8.4
118.83	25.79	10.3	8.7
126.31	21.92	11.0	9.5
133.78	23.40	8.6	11.0

$E_n = 5.50 \pm 0.09$ MeV
(n,n') to: 3.198 MeV Level

θ_{cm} deg.	$d\sigma/d\omega$ mb/str	Δ (%)	
		+	-
27.69	12.29	27.2	17.8
42.79	9.59	23.8	19.1
47.82	11.86	36.1	16.5
55.36	17.15	11.0	15.0
62.88	8.64	42.5	18.2
70.40	14.70	17.0	20.4
77.92	11.27	22.3	18.2
107.91	9.94	20.3	17.2
126.35	11.03	14.2	14.6

Avg. $d\sigma/d\omega = 11.69 \text{ mb/str} \pm 10.7 \%$
 $\int(d\sigma/d\omega)d\omega = 146.88 \text{ mb} \pm 10.7 \%$

$E_n = 5.50 \pm 0.09$ MeV
(n,n') to: 3.475 MeV Level

θ_{cm} deg.	$d\sigma/d\omega$ mb/str	Δ (%)	
		+	-
27.71	10.98	30.1	20.5
42.81	8.12	38.0	22.6
47.84	11.62	20.1	24.9
55.38	14.08	16.0	20.5
62.90	11.23	19.9	22.5
70.43	15.05	11.0	23.9
77.95	12.08	28.7	22.2

Avg. $d\sigma/d\omega = 11.77$ mb/str $\pm 12.7\%$
 $\int(d\sigma/d\omega)d\omega = 147.94$ mb $\pm 12.7\%$

$E_n = 5.50 \pm 0.09$ MeV
(n,n') to: 3.708 MeV Level

θ_{cm} deg.	$d\sigma/d\omega$ mb/str	Δ (%)	
		+	-
42.83	6.10	39.1	30.3

Avg. $d\sigma/d\omega = 6.10$ mb/str $\pm 35.4\%$
 $\int(d\sigma/d\omega)d\omega = 76.63$ mb $\pm 35.4\%$

$E_n = 5.50 \pm 0.09$ MeV
(n,n') to: 3.961 MeV Level
+ 4.076 MeV Level
+ 4.323 MeV Level

θ_{cm} deg.	$d\sigma/d\omega$ mb/str	Δ (%)	
		+	-
27.76	99.04	9.6	10.6
35.33	100.05	10.3	14.0
42.88	99.48	8.2	12.1
47.92	96.25	9.7	15.8
55.47	114.73	8.3	13.7
62.99	104.76	8.4	13.9
70.53	104.71	9.2	17.0
78.05	109.81	8.4	16.1
85.56	106.15	8.2	14.5
93.07	109.94	8.0	11.9
100.56	106.32	8.1	12.0
108.04	104.33	8.9	16.3
119.00	103.45	8.1	15.1
126.46	104.07	9.6	14.7
133.91	91.83	8.7	11.6

Avg. $d\sigma/d\omega = 99.14$ mb/str $\pm 10.4\%$
 $\int(d\sigma/d\omega)d\omega = 1245.80$ mb $\pm 10.4\%$

$E_n = 7.00 \pm 0.06$ MeV
Elastic Scattering

θ_{cm} deg.	$d\sigma/d\omega$ mb/str	Δ (%)	
		+	-
13.00	5242.15	3.9	5.0
17.59	2845.98	5.4	4.6
27.63	1090.81	5.6	4.8
28.00	1075.00	6.2	6.0
30.64	738.01	5.1	5.1
35.17	363.26	5.3	5.4
38.17	252.97	7.0	6.7
42.69	178.87	7.0	5.2
45.71	144.97	7.5	10.0
47.70	146.54	6.1	6.2
51.72	97.70	8.6	7.4
55.23	65.01	8.2	9.1
59.24	25.61	13.1	13.0
62.75	15.73	22.0	15.5
66.76	28.24	16.8	12.9
70.26	62.55	11.5	7.0
77.77	142.88	5.7	5.8
82.77	149.17	7.9	4.8
85.28	146.34	7.3	5.0
90.27	120.25	6.9	5.5
92.78	100.53	5.2	5.7
97.78	52.57	10.9	6.8
100.27	37.84	12.2	8.4
107.77	19.15	14.4	15.9
118.74	40.53	8.8	7.1
126.23	58.87	8.0	6.4
133.70	40.52	12.8	7.1

$\int(d\sigma/d\omega)d\omega = 3401.95 \text{ mb} \pm 7.3 \%$
Wick's Limit = $7128.25 \text{ mb} \pm 7.3 \%$
 $\sigma_T = 5.80 \text{ b} \pm 1.0 \%$

Legendre Fit, Order = 12

k	a_k	Δ (%)
0	541.43701	1.9
1	411.00073	2.4
2	335.26685	2.7
3	284.73389	2.8
4	233.77351	2.9
5	170.42192	3.5
6	108.93321	4.5
7	68.77304	5.8
8	53.93671	5.7
9	33.22380	6.8
10	9.93364	17.7
11	1.82599	60.9
12	-1.08286	80.5

$E_n = 7.00 \pm 0.06$ MeV
(n,n') to: 2.615 MeV Level

θ_{cm} deg.	$d\sigma/d\omega$ mb/str	Δ (%)	
		+	-
35.21	13.00	31.5	16.5
42.74	14.09	19.9	18.6
47.76	11.30	14.7	10.6
55.29	12.35	10.1	9.7
59.30	13.72	9.2	9.2
62.82	11.17	7.4	11.6
66.82	10.24	11.8	12.2
70.34	10.30	13.4	10.3
77.85	9.48	11.3	10.2
82.85	10.46	17.4	10.3
85.35	9.06	13.3	12.0
90.35	9.31	18.4	13.7
92.85	11.11	10.8	10.7
97.85	10.90	12.5	10.3
100.35	9.80	9.4	10.8
107.84	8.86	11.9	13.8
118.81	8.18	34.2	9.7
126.29	9.69	12.8	15.0
133.76	6.55	13.2	11.8

$E_n = 7.00 \pm 0.06$ MeV
(n,n') to: 3.198 MeV Level

θ_{cm} deg.	$d\sigma/d\omega$ mb/str	Δ (%)	
		+	-
77.86	4.82	15.7	20.9
82.87	5.12	21.7	25.9
90.38	3.41	34.3	14.8
92.88	3.85	28.7	21.8
97.87	4.20	27.5	23.5
100.37	3.90	25.1	28.7
126.31	3.59	14.0	21.5

Avg. $d\sigma/d\omega = 3.92 \text{ mb/str} \pm 11.6 \%$
 $\int(d\sigma/d\omega)d\omega = 49.28 \text{ mb} \pm 11.6 \%$

$E_n = 7.00 \pm 0.06$ MeV
(n,n') to: 3.475 MeV Level

θ_{cm} deg.	$d\sigma/d\omega$ mb/str	Δ (%)	
		+	-
77.88	3.96	14.2	17.5
82.89	4.26	29.4	26.1
90.39	2.67	53.1	31.0
92.89	3.16	20.2	20.9
97.89	4.31	24.9	20.2
100.39	4.00	12.1	26.0

Avg. $d\sigma/d\omega = 3.73$ mb/str ± 12.3 %
 $\int(d\sigma/d\omega)d\omega = 46.92$ mb ± 12.3 %

$E_n = 7.00 \pm 0.06$ MeV
(n,n') to: 3.708 MeV Level

θ_{cm} deg.	$d\sigma/d\omega$ mb/str	Δ (%)	
		+	-
77.90	4.40	12.0	22.5
82.90	4.22	27.3	20.7
90.40	5.44	23.6	13.8

Avg. $d\sigma/d\omega = 4.68$ mb/str ± 11.5 %
 $\int(d\sigma/d\omega)d\omega = 58.78$ mb ± 11.5 %

$E_n = 7.00 \pm 0.06$ MeV
(n,n') to: 3.961 MeV Level
+ 4.076 MeV Level

θ_{cm} deg.	$d\sigma/d\omega$ mb/str	Δ (%)	
		+	-
82.92	23.43	12.7	15.7
90.42	22.80	15.1	17.3
92.93	22.75	13.0	20.0
97.92	23.14	11.4	22.3

Avg. $d\sigma/d\omega = 22.97$ mb/str ± 11.1 %
 $\int(d\sigma/d\omega)d\omega = 288.58$ mb ± 11.1 %

$E_n = 7.00 \pm 0.06$ MeV
(n,n') to: 3.961 MeV Level
+ 4.076 MeV Level
+ 4.323 MeV Level

θ_{cm} deg.	$d\sigma/d\omega$ mb/str	Δ (%)	
		+	-
27.70	61.61	9.8	15.9
35.25	50.55	14.3	13.9
42.80	53.61	8.3	17.5
47.83	58.40	6.7	15.7
55.36	61.30	5.5	15.5
62.89	51.51	5.8	13.3
66.90	52.98	6.6	15.5
70.42	56.86	5.5	13.8
77.93	54.47	5.4	12.9
82.94	58.11	6.6	7.8
85.44	53.07	6.3	15.1
90.43	54.77	8.3	7.7
92.94	54.39	5.8	9.0
97.93	56.65	7.1	13.4
100.44	55.61	5.3	12.3
107.92	51.13	5.5	8.2
118.88	52.75	5.8	10.6
126.36	53.43	5.3	10.9
133.82	48.79	5.5	13.8

Avg. $d\sigma/d\omega = 51.64$ mb/str ± 8.6 %
 $\int(d\sigma/d\omega)d\omega = 648.96$ mb ± 8.6 %

$E_n = 7.00 \pm 0.06$ MeV
(n,n') to: 4.323 MeV Level

θ_{cm} deg.	$d\sigma/d\omega$ mb/str	Δ (%)	
		+	-
82.94	34.50	9.8	14.0
90.45	34.95	6.9	16.7
92.95	30.79	9.1	16.5
97.94	33.78	10.0	19.1

Avg. $d\sigma/d\omega = 32.18$ mb/str ± 10.3 %
 $\int(d\sigma/d\omega)d\omega = 404.41$ mb ± 10.3 %

$E_n = 7.00 \pm 0.06$ MeV
(n,n') to: 4.698 MeV Level

θ_{cm} deg.	$d\sigma/d\omega$ mb/str	Δ (%)	
		+	-
82.98	11.54	14.6	17.4
90.48	13.52	16.1	21.7
92.99	12.23	15.3	16.3
97.98	11.56	26.9	26.1
100.48	12.01	9.2	23.8
118.93	9.75	14.0	27.1
126.39	11.19	11.1	18.3

Avg. $d\sigma/d\omega = 11.14$ mb/str ± 11.0 %
 $\int(d\sigma/d\omega)d\omega = 140.02$ mb ± 11.0 %

$E_n = 7.00 \pm 0.06$ MeV
(n,n') to: 4.974 MeV Level
+ 5.038 MeV Level

θ_{cm} deg.	$d\sigma/d\omega$ mb/str	Δ (%)	
		+	-
83.01	14.50	12.3	26.0
90.51	22.04	15.5	19.0
93.02	21.36	10.0	22.0
98.01	22.97	11.7	23.6
100.51	20.39	19.1	17.9
118.95	19.65	18.8	24.6
126.42	22.38	14.2	13.7

Avg. $d\sigma/d\omega = 18.04$ mb/str ± 11.1 %
 $\int(d\sigma/d\omega)d\omega = 226.68$ mb ± 11.1 %

$E_n = 7.00 \pm 0.06$ MeV
(n,n') to: 5.254 MeV Level

θ_{cm} deg.	$d\sigma/d\omega$ mb/str	Δ (%)	
		+	-
83.04	19.54	15.5	26.6
90.55	21.71	22.6	23.1
93.06	29.72	12.1	20.2
98.04	24.09	20.9	19.1
100.55	24.81	10.1	23.9
118.99	16.97	34.7	19.0

Avg. $d\sigma/d\omega = 21.85$ mb/str ± 12.3 %
 $\int(d\sigma/d\omega)d\omega = 274.50$ mb ± 12.3 %

$E_n = 8.50 \pm 0.04$ MeV
Elastic Scattering

θ_{cm} deg.	$d\sigma/d\omega$ mb/str	Δ (%)	
		+	-
13.00	4033.67	6.0	4.6
20.50	1684.41	5.5	5.4
27.63	482.16	5.0	5.5
28.00	446.83	9.7	11.2
35.16	199.15	5.4	5.4
42.68	244.28	5.3	7.2
47.70	166.69	5.9	7.4
47.70	179.88	6.2	6.0
55.22	76.60	9.0	7.6
55.23	65.88	9.3	8.8
62.75	26.76	12.0	13.2
62.75	27.97	14.2	12.4
70.26	93.30	7.7	7.0
77.77	135.26	7.9	5.6
85.27	111.04	10.6	5.6
92.78	60.19	7.3	7.6
100.27	23.25	11.7	12.0
107.77	28.85	11.3	12.6
118.74	53.25	8.2	8.4
126.23	45.80	9.9	7.6
133.70	23.79	11.2	11.0

$\int(d\sigma/d\omega)d\omega = 2726.34$ mb ± 7.4 %
Wick's Limit = 7227.69 mb ± 8.1 %
 $\sigma_T = 5.30$ b ± 2.0 %

Legendre Fit, Order = 12

k	a_k	Δ (%)
0	433.91016	2.2
1	320.86353	2.9
2	257.88721	3.3
3	222.77199	3.5
4	190.94403	3.5
5	153.77766	3.8
6	115.56726	4.2
7	83.61865	4.9
8	69.21420	4.6
9	54.05298	4.4
10	28.53816	6.6
11	11.36589	10.9
12	3.27083	26.9

$E_n = 8.50 \pm 0.04$ MeV
(n,n') to: 2.615 MeV Level

θ_{cm} deg.	$d\sigma/d\omega$ mb/str	Δ (%)	
		+	-
47.75	7.92	23.6	8.7
47.75	8.05	26.3	16.7
55.27	8.42	15.2	14.2
55.28	8.07	14.4	18.0
62.80	7.70	15.8	18.0
62.80	7.38	19.0	17.4
70.31	6.85	13.8	16.7
77.82	6.57	21.4	16.4
92.84	6.07	29.3	22.4
100.33	7.82	16.8	11.8
118.80	4.52	31.4	22.3
126.27	4.34	24.8	24.3
133.74	4.35	26.4	18.2

$E_n = 8.50 \pm 0.04$ MeV
(n,n') to: 4.076 MeV Level
+ 4.323 MeV Level

θ_{cm} deg.	$d\sigma/d\omega$ mb/str	Δ (%)	
		+	-
55.33	19.28	4.5	4.5
55.33	19.79	11.0	20.7
62.85	17.39	11.4	24.0
77.88	17.55	8.1	18.5
92.89	17.19	8.6	19.3
107.88	16.28	7.4	17.4
118.85	16.07	7.6	19.4

Avg. $d\sigma/d\omega = 18.44$ mb/str ± 8.3 %
 $\int(d\sigma/d\omega)d\omega = 231.76$ mb ± 8.3 %

$E_n = 6.00 \pm 0.04$ MeV
(n,n') to: 2.615 MeV Level

θ_{cm} deg.	$d\sigma/d\omega$ mb/str	Δ (%)	
		+	-
82.87	15.30	9.3	9.4
90.37	14.60	9.4	7.9
97.86	16.79	13.3	8.4

$E_n = 8.50 \pm 0.04$ MeV
(n,n') to: 3.961 MeV Level
+ 4.076 MeV Level
+ 4.323 MeV Level

θ_{cm} deg.	$d\sigma/d\omega$ mb/str	Δ (%)	
		+	-
47.79	22.81	11.8	15.6
47.79	24.19	8.5	18.9
55.33	18.54	15.3	15.3
70.37	18.42	9.3	18.5
100.39	19.45	6.1	12.8
126.32	17.85	7.4	13.2
133.79	18.02	8.8	11.8

Avg. $d\sigma/d\omega = 18.51$ mb/str ± 8.9 %
 $\int(d\sigma/d\omega)d\omega = 232.62$ mb ± 8.9 %

$E_n = 6.00 \pm 0.04$ MeV
(n,n') to: 3.198 MeV Level

θ_{cm} deg.	$d\sigma/d\omega$ mb/str	Δ (%)	
		+	-
82.90	11.06	8.2	16.2
90.41	10.25	9.9	10.2
97.90	9.89	10.0	14.3

Avg. $d\sigma/d\omega = 10.18$ mb/str ± 10.3 %
 $\int(d\sigma/d\omega)d\omega = 127.93$ mb ± 10.3 %

$E_n = 6.00 \pm 0.04$ MeV
(n,n') to: 3.475 MeV Level

θ_{cm} deg.	$d\sigma/d\omega$ mb/str	Δ (%)	
		+	-
82.93	11.13	16.8	9.4
90.43	9.87	20.9	7.1
97.92	10.62	9.2	9.8

Avg. $d\sigma/d\omega = 10.77$ mb/str ± 10.1 %
 $\int(d\sigma/d\omega)d\omega = 135.33$ mb ± 10.1 %

$E_n = 6.00 \pm 0.04$ MeV
(n,n') to: 3.708 MeV Level

θ_{cm} deg.	$d\sigma/d\omega$ mb/str	Δ (%)	
		+	-
82.95	8.75	14.6	7.9
90.44	7.69	26.0	9.0
97.94	9.42	9.1	8.9

Avg. $d\sigma/d\omega = 9.12$ mb/str ± 10.7 %
 $\int(d\sigma/d\omega)d\omega = 114.62$ mb ± 10.7 %

$E_n = 6.00 \pm 0.04$ MeV
(n,n') to: 3.961 MeV Level
+ 4.076 MeV Level

θ_{cm} deg.	$d\sigma/d\omega$ mb/str	Δ (%)	
		+	-
82.98	42.12	11.8	11.3
90.48	41.80	12.1	6.8
97.98	43.92	8.6	8.4

Avg. $d\sigma/d\omega = 43.12$ mb/str ± 10.4 %
 $\int(d\sigma/d\omega)d\omega = 541.87$ mb ± 10.4 %

$E_n = 6.00 \pm 0.04$ MeV
(n,n') to: 3.961 MeV Level
+ 4.076 MeV Level
+ 4.323 MeV Level

θ_{cm} deg.	$d\sigma/d\omega$ mb/str	Δ (%)	
		+	-
83.00	93.30	6.4	7.4
90.50	90.97	7.4	6.4
98.00	92.28	6.5	6.5

Avg. $d\sigma/d\omega = 92.21$ mb/str ± 9.5 %
 $\int(d\sigma/d\omega)d\omega = 1158.72$ mb ± 9.5 %

$E_n = 6.00 \pm 0.04$ MeV
(n,n') to: 4.323 MeV Level

θ_{cm} deg.	$d\sigma/d\omega$ mb/str	Δ (%)	
		+	-
83.02	51.77	7.4	16.5
90.53	49.04	7.5	13.5
98.02	47.77	7.9	16.7

Avg. $d\sigma/d\omega = 48.24$ mb/str ± 10.3 %
 $\int(d\sigma/d\omega)d\omega = 606.13$ mb ± 10.3 %

$E_n = 6.00 \pm 0.04$ MeV
(n,n') to: 4.698 MeV Level

θ_{cm} deg.	$d\sigma/d\omega$ mb/str	Δ (%)	
		+	-
83.11	15.47	14.9	20.3
90.60	16.08	10.3	14.3
98.09	16.98	10.3	13.1

Avg. $d\sigma/d\omega = 16.16$ mb/str ± 11.6 %
 $\int(d\sigma/d\omega)d\omega = 203.11$ mb ± 11.6 %

$E_n = 6.00 \pm 0.04$ MeV
(n,n') to: 4.974 MeV Level
+ 5.038 MeV Level

θ_{cm} deg.	$d\sigma/d\omega$ mb/str	Δ (%)	
		+	-
83.17	31.93	13.2	16.4
90.68	35.47	12.6	15.1
98.17	31.25	13.4	15.7

Avg. $d\sigma/d\omega = 32.29$ mb/str $\pm 13.7\%$
 $\int(d\sigma/d\omega)d\omega = 405.80$ mb $\pm 13.7\%$

$E_n = 6.49 \pm 0.03$ MeV
(n,n') to: 3.708 MeV Level

θ_{cm} deg.	$d\sigma/d\omega$ mb/str	Δ (%)	
		+	-
82.92	6.57	20.7	13.9
90.42	5.53	15.0	7.9
97.92	5.78	14.4	27.6

Avg. $d\sigma/d\omega = 5.93$ mb/str $\pm 11.6\%$
 $\int(d\sigma/d\omega)d\omega = 74.48$ mb $\pm 11.6\%$

$E_n = 6.49 \pm 0.03$ MeV
(n,n') to: 2.615 MeV Level

θ_{cm} deg.	$d\sigma/d\omega$ mb/str	Δ (%)	
		+	-
82.85	10.62	20.0	9.0
90.36	11.26	10.7	9.1
97.85	11.60	10.7	8.8

$E_n = 6.49 \pm 0.03$ MeV
(n,n') to: 3.961 MeV Level
+ 4.076 MeV Level

θ_{cm} deg.	$d\sigma/d\omega$ mb/str	Δ (%)	
		+	-
82.94	36.91	15.3	9.8
90.45	36.34	12.1	9.5
97.94	34.86	9.6	9.9

Avg. $d\sigma/d\omega = 35.98$ mb/str $\pm 9.7\%$
 $\int(d\sigma/d\omega)d\omega = 452.08$ mb $\pm 9.7\%$

$E_n = 6.49 \pm 0.03$ MeV
(n,n') to: 3.198 MeV Level

θ_{cm} deg.	$d\sigma/d\omega$ mb/str	Δ (%)	
		+	-
82.88	6.10	16.0	7.5
90.39	6.33	14.0	12.1
97.88	6.42	10.5	18.0

Avg. $d\sigma/d\omega = 6.28$ mb/str $\pm 11.5\%$
 $\int(d\sigma/d\omega)d\omega = 78.91$ mb $\pm 11.5\%$

$E_n = 6.49 \pm 0.03$ MeV
(n,n') to: 3.961 MeV Level
+ 4.076 MeV Level
+ 4.323 MeV Level

θ_{cm} deg.	$d\sigma/d\omega$ mb/str	Δ (%)	
		+	-
82.96	77.07	7.1	5.6
90.46	78.24	6.7	6.1
97.96	76.52	5.4	12.4

Avg. $d\sigma/d\omega = 76.96$ mb/str $\pm 8.7\%$
 $\int(d\sigma/d\omega)d\omega = 967.09$ mb $\pm 8.7\%$

$E_n = 6.49 \pm 0.03$ MeV
(n,n') to: 3.475 MeV Level

θ_{cm} deg.	$d\sigma/d\omega$ mb/str	Δ (%)	
		+	-
82.90	4.64	19.8	10.6
90.41	6.15	16.3	8.0
97.90	5.71	8.5	24.6

Avg. $d\sigma/d\omega = 5.81$ mb/str $\pm 9.5\%$
 $\int(d\sigma/d\omega)d\omega = 72.96$ mb $\pm 9.5\%$

$E_n = 6.49 \pm 0.03$ MeV
(n,n') to: 4.323 MeV Level

θ_{cm} deg.	$d\sigma/d\omega$ mb/str	Δ (%)	
		+	-
82.97	42.14	7.7	12.7
90.48	43.64	8.7	14.9
97.97	39.92	7.7	11.0

Avg. $d\sigma/d\omega = 40.61$ mb/str ± 10.0 %
 $\int(d\sigma/d\omega)d\omega = 510.25$ mb ± 10.0 %

$E_n = 6.49 \pm 0.03$ MeV
(n,n') to: 5.254 MeV Level

θ_{cm} deg.	$d\sigma/d\omega$ mb/str	Δ (%)	
		+	-
83.14	29.31	14.4	15.5
90.64	33.06	12.4	11.4
98.13	29.59	11.2	18.8

Avg. $d\sigma/d\omega = 30.74$ mb/str ± 11.7 %
 $\int(d\sigma/d\omega)d\omega = 386.27$ mb ± 11.7 %

$E_n = 6.49 \pm 0.03$ MeV
(n,n') to: 4.698 MeV Level

θ_{cm} deg.	$d\sigma/d\omega$ mb/str	Δ (%)	
		+	-
83.03	13.17	17.2	17.7
90.53	14.40	17.5	12.9
98.02	13.21	13.3	23.9

Avg. $d\sigma/d\omega = 13.64$ mb/str ± 11.8 %
 $\int(d\sigma/d\omega)d\omega = 171.46$ mb ± 11.8 %

$E_n = 7.50 \pm 0.03$ MeV
(n,n') to: 2.615 MeV Level

θ_{cm} deg.	$d\sigma/d\omega$ mb/str	Δ (%)	
		+	-
82.85	7.21	27.1	8.1
90.34	8.23	13.5	7.9
97.85	9.29	9.1	10.7

Avg. $d\sigma/d\omega = 8.11$ mb/str ± 11.8 %
 $\int(d\sigma/d\omega)d\omega = 100.00$ mb ± 11.8 %

$E_n = 6.49 \pm 0.03$ MeV
(n,n') to: 4.974 MeV Level
+ 5.038 MeV Level

θ_{cm} deg.	$d\sigma/d\omega$ mb/str	Δ (%)	
		+	-
83.07	29.46	10.8	13.2
90.57	30.96	11.9	11.2
98.06	24.21	7.1	25.1

Avg. $d\sigma/d\omega = 24.86$ mb/str ± 9.9 %
 $\int(d\sigma/d\omega)d\omega = 312.33$ mb ± 9.9 %

$E_n = 7.50 \pm 0.03$ MeV
(n,n') to: 3.198 MeV Level

θ_{cm} deg.	$d\sigma/d\omega$ mb/str	Δ (%)	
		+	-
82.87	3.19	28.4	23.0
90.37	3.80	22.8	16.7
97.87	2.94	25.2	31.8

Avg. $d\sigma/d\omega = 3.39$ mb/str ± 14.7 %
 $\int(d\sigma/d\omega)d\omega = 42.57$ mb ± 14.7 %

$E_n = 7.50 \pm 0.03$ MeV
(n,n') to: 3.475 MeV Level

θ_{cm} deg.	$d\sigma/d\omega$ mb/str	Δ (%)	
		+	-
90.38	2.14	41.6	30.8
97.88	2.42	18.0	33.9

Avg. $d\sigma/d\omega = 2.29$ mb/str ± 27.4 %
 $\int(d\sigma/d\omega)d\omega = 28.78$ mb ± 27.4 %

$E_n = 7.50 \pm 0.03$ MeV
(n,n') to: 3.708 MeV Level

θ_{cm} deg.	$d\sigma/d\omega$ mb/str	Δ (%)	
		+	-
90.39	2.44	30.8	27.5
97.89	2.62	27.0	30.4

Avg. $d\sigma/d\omega = 2.52$ mb/str ± 22.9 %
 $\int(d\sigma/d\omega)d\omega = 31.69$ mb ± 22.9 %

$E_n = 7.50 \pm 0.03$ MeV
(n,n') to: 3.961 MeV Level
+ 4.076 MeV Level
+ 4.323 MeV Level

θ_{cm} deg.	$d\sigma/d\omega$ mb/str	Δ (%)	
		+	-
82.92	38.72	7.4	8.1
90.42	37.58	7.7	9.2
97.91	38.21	5.2	14.7

Avg. $d\sigma/d\omega = 38.10$ mb/str ± 9.3 %
 $\int(d\sigma/d\omega)d\omega = 478.82$ mb ± 9.3 %

$E_n = 7.50 \pm 0.03$ MeV
(n,n') to: 4.698 MeV Level

θ_{cm} deg.	$d\sigma/d\omega$ mb/str	Δ (%)	
		+	-
82.95	9.38	20.6	25.3
90.46	8.77	21.8	26.3
97.95	8.19	13.1	31.8

Avg. $d\sigma/d\omega = 8.43$ mb/str ± 13.2 %
 $\int(d\sigma/d\omega)d\omega = 105.95$ mb ± 13.2 %

$E_n = 7.50 \pm 0.03$ MeV
(n,n') to: 4.974 MeV Level
+ 5.038 MeV Level

θ_{cm} deg.	$d\sigma/d\omega$ mb/str	Δ (%)	
		+	-
82.98	16.88	11.4	23.6
90.48	16.82	11.0	21.9
97.97	17.23	7.0	24.8

Avg. $d\sigma/d\omega = 16.87$ mb/str ± 12.0 %
 $\int(d\sigma/d\omega)d\omega = 212.05$ mb ± 12.0 %

$E_n = 7.50 \pm 0.03$ MeV
(n,n') to: 5.254 MeV Level

θ_{cm} deg.	$d\sigma/d\omega$ mb/str	Δ (%)	
		+	-
83.00	20.57	12.6	36.3
90.51	18.05	27.0	11.8
98.01	18.44	25.8	19.3

Avg. $d\sigma/d\omega = 18.64$ mb/str ± 18.5 %
 $\int(d\sigma/d\omega)d\omega = 234.24$ mb ± 18.5 %

$E_n = 8.01 \pm 0.03$ MeV
(n,n') to: 2.615 MeV Level

θ_{cm} deg.	$d\sigma/d\omega$ mb/str	Δ (%)	
		+	-
82.83	8.15	22.0	10.8
90.33	7.02	23.6	9.5
97.84	8.73	15.6	17.5

$E_n = 8.01 \pm 0.03$ MeV
(n,n') to: 3.198 MeV Level

θ_{cm} deg.	$d\sigma/d\omega$ mb/str	Δ (%)	
		+	-
82.85	2.69	40.4	25.2
90.35	3.06	26.1	25.9

Avg. $d\sigma/d\omega = 2.94$ mb/str ± 23.1 %
 $\int(d\sigma/d\omega)d\omega = 36.89$ mb ± 23.1 %

$E_n = 8.01 \pm 0.03$ MeV
(n,n') to: 3.475 MeV Level

θ_{cm} deg.	$d\sigma/d\omega$ mb/str	Δ (%)	
		+	-
82.87	2.51	39.5	20.0
90.37	1.47	52.5	32.9
97.87	1.61	28.9	29.2

Avg. $d\sigma/d\omega = 1.94$ mb/str $\pm 17.8\%$
 $\int(d\sigma/d\omega)d\omega = 24.37$ mb $\pm 17.8\%$

$E_n = 8.01 \pm 0.03$ MeV
(n,n') to: 3.708 MeV Level

θ_{cm} deg.	$d\sigma/d\omega$ mb/str	Δ (%)	
		+	-
82.88	1.50	43.6	28.4
90.38	2.08	40.5	31.0

Avg. $d\sigma/d\omega = 1.80$ mb/str $\pm 26.7\%$
 $\int(d\sigma/d\omega)d\omega = 22.56$ mb $\pm 26.7\%$

$E_n = 8.01 \pm 0.03$ MeV
(n,n') to: 3.961 MeV Level
+ 4.076 MeV Level
+ 4.323 MeV Level

θ_{cm} deg.	$d\sigma/d\omega$ mb/str	Δ (%)	
		+	-
82.90	27.82	9.7	8.3
90.40	28.90	8.7	10.1
97.89	27.27	5.7	7.9

Avg. $d\sigma/d\omega = 27.56$ mb/str $\pm 8.7\%$
 $\int(d\sigma/d\omega)d\omega = 346.37$ mb $\pm 8.7\%$

$E_n = 8.01 \pm 0.03$ MeV
(n,n') to: 4.698 MeV Level

θ_{cm} deg.	$d\sigma/d\omega$ mb/str	Δ (%)	
		+	-
90.43	6.69	16.6	22.4
97.93	5.28	16.9	31.1

Avg. $d\sigma/d\omega = 5.64$ mb/str $\pm 15.5\%$
 $\int(d\sigma/d\omega)d\omega = 70.83$ mb $\pm 15.5\%$

$E_n = 8.01 \pm 0.03$ MeV
(n,n') to: 4.974 MeV Level
+ 5.038 MeV Level

θ_{cm} deg.	$d\sigma/d\omega$ mb/str	Δ (%)	
		+	-
90.44	8.26	18.6	23.8
97.94	10.78	10.1	15.4

Avg. $d\sigma/d\omega = 9.43$ mb/str $\pm 14.2\%$
 $\int(d\sigma/d\omega)d\omega = 118.50$ mb $\pm 14.2\%$

$E_n = 8.01 \pm 0.03$ MeV
(n,n') to: 5.254 MeV Level

θ_{cm} deg.	$d\sigma/d\omega$ mb/str	Δ (%)	
		+	-
90.47	14.28	18.7	23.8
97.97	14.52	17.2	25.3

Avg. $d\sigma/d\omega = 14.36$ mb/str $\pm 16.9\%$
 $\int(d\sigma/d\omega)d\omega = 180.45$ mb $\pm 16.9\%$

²⁰⁷Pb CROSS SECTIONS

$E_n = 5.50 \pm 0.00$ MeV
(n,n') to: 0.570 MeV Level

θ_{cm} deg.	$d\sigma/d\omega$ mb/str	Δ (%)	
		+	-
90.29	7.15	22.0	32.5
97.79	4.56	40.9	29.2

$E_n = 5.50 \pm 0.00$ MeV
(n,n') to: 0.898 MeV Level

θ_{cm} deg.	$d\sigma/d\omega$ mb/str	Δ (%)	
		+	-
90.31	5.52	29.9	21.0
97.81	3.15	64.5	31.9

Avg. $d\sigma/d\omega = 4.95$ mb/str ± 21.6 %
 $\int(d\sigma/d\omega)d\omega = 62.24$ mb ± 21.6 %

$E_n = 5.50 \pm 0.00$ MeV
(n,n') to: 1.633 MeV Level

θ_{cm} deg.	$d\sigma/d\omega$ mb/str	Δ (%)	
		+	-
90.33	2.24	58.5	23.3
97.83	3.72	17.4	30.8

Avg. $d\sigma/d\omega = 3.08$ mb/str ± 29.0 %
 $\int(d\sigma/d\omega)d\omega = 38.75$ mb ± 29.0 %

$E_n = 5.50 \pm 0.00$ MeV
(n,n') to: 2.340 MeV Level

θ_{cm} deg.	$d\sigma/d\omega$ mb/str	Δ (%)	
		+	-
82.87	4.63	20.9	23.4
90.37	4.43	16.9	10.9
97.87	5.08	13.2	11.8

Avg. $d\sigma/d\omega = 4.80$ mb/str ± 11.8 %
 $\int(d\sigma/d\omega)d\omega = 60.38$ mb ± 11.8 %

$E_n = 5.50 \pm 0.00$ MeV
(n,n') to: 2.624 MeV Level
+ 2.662 MeV Level

θ_{cm} deg.	$d\sigma/d\omega$ mb/str	Δ (%)	
		+	-
82.88	14.75	11.8	11.7
90.39	14.29	9.3	8.4
97.89	14.74	9.5	15.0

Avg. $d\sigma/d\omega = 14.49$ mb/str ± 10.3 %
 $\int(d\sigma/d\omega)d\omega = 182.12$ mb ± 10.3 %

$E_n = 5.50 \pm 0.00$ MeV
(n,n') to: 3.202 MeV Level
+ 3.222 MeV Level

θ_{cm} deg.	$d\sigma/d\omega$ mb/str	Δ (%)	
		+	-
82.93	12.22	11.6	16.1
90.43	11.29	24.9	13.7
97.93	13.41	9.4	18.3

Avg. $d\sigma/d\omega = 12.32$ mb/str ± 12.1 %
 $\int(d\sigma/d\omega)d\omega = 154.76$ mb ± 12.1 %

$E_n = 5.50 \pm 0.00$ MeV
(n,n') to: 3.202 MeV Level
+ 3.222 MeV Level
+ 3.450 MeV Level
+ 3.600 MeV Level

θ_{cm} deg.	$d\sigma/d\omega$ mb/str	Δ (%)	
		+	-
82.96	43.20	9.2	7.2
97.96	47.94	7.1	9.7

Avg. $d\sigma/d\omega = 45.11$ mb/str ± 10.6 %
 $\int(d\sigma/d\omega)d\omega = 566.91$ mb ± 10.6 %

$E_n = 5.50 \pm 0.00$ MeV
 (n,n') to: 3.202 MeV Level
 + 3.222 MeV Level
 + 3.450 MeV Level
 + 3.600 MeV Level
 + 3.776 MeV Level

θ_{cm} deg.	$d\sigma/d\omega$ mb/str	Δ (%)	
		+	-
90.46	43.93	9.6	11.3

Avg. $d\sigma/d\omega = 43.93$ mb/str $\pm 12.6\%$
 $\int(d\sigma/d\omega)d\omega = 552.07$ mb $\pm 12.6\%$

$E_n = 5.50 \pm 0.00$ MeV
 (n,n') to: 3.450 MeV Level

θ_{cm} deg.	$d\sigma/d\omega$ mb/str	Δ (%)	
		+	-
82.96	16.81	19.1	20.5
90.46	17.42	10.1	21.7

Avg. $d\sigma/d\omega = 17.06$ mb/str $\pm 16.6\%$
 $\int(d\sigma/d\omega)d\omega = 214.39$ mb $\pm 16.6\%$

$E_n = 5.50 \pm 0.00$ MeV
 (n,n') to: 3.450 MeV Level
 + 3.600 MeV Level

θ_{cm} deg.	$d\sigma/d\omega$ mb/str	Δ (%)	
		+	-
97.97	33.55	8.3	9.9

Avg. $d\sigma/d\omega = 33.55$ mb/str $\pm 11.5\%$
 $\int(d\sigma/d\omega)d\omega = 421.63$ mb $\pm 11.5\%$

$E_n = 5.50 \pm 0.00$ MeV
 (n,n') to: 3.600 MeV Level

θ_{cm} deg.	$d\sigma/d\omega$ mb/str	Δ (%)	
		+	-
82.98	13.87	16.6	18.0

Avg. $d\sigma/d\omega = 13.87$ mb/str $\pm 18.7\%$
 $\int(d\sigma/d\omega)d\omega = 174.30$ mb $\pm 18.7\%$

$E_n = 5.50 \pm 0.00$ MeV
 (n,n') to: 3.776 MeV Level

θ_{cm} deg.	$d\sigma/d\omega$ mb/str	Δ (%)	
		+	-
83.02	13.27	14.1	23.5

Avg. $d\sigma/d\omega = 13.27$ mb/str $\pm 20.0\%$
 $\int(d\sigma/d\omega)d\omega = 166.78$ mb $\pm 20.0\%$

$E_n = 5.50 \pm 0.00$ MeV
 (n,n') to: 4.128 MeV Level
 + 4.368 MeV Level
 + 4.386 MeV Level

θ_{cm} deg.	$d\sigma/d\omega$ mb/str	Δ (%)	
		+	-
83.10	53.76	10.6	11.9

Avg. $d\sigma/d\omega = 53.76$ mb/str $\pm 13.3\%$
 $\int(d\sigma/d\omega)d\omega = 675.49$ mb $\pm 13.3\%$

$E_n = 6.00 \pm 0.00$ MeV
 (n,n') to: 0.570 MeV Level

θ_{cm} deg.	$d\sigma/d\omega$ mb/str	Δ (%)	
		+	-
97.80	0.77	****	36.7

$E_n = 6.00 \pm 0.00$ MeV
 (n,n') to: 0.898 MeV Level

θ_{cm} deg.	$d\sigma/d\omega$ mb/str	Δ (%)	
		+	-
97.80	1.03	****	28.6

Avg. $d\sigma/d\omega = 1.03$ mb/str $\pm 84.8\%$
 $\int(d\sigma/d\omega)d\omega = 13.00$ mb $\pm 84.8\%$

$E_n = 6.00 \pm 0.00$ MeV
(n,n') to: 1.633 MeV Level

θ_{cm} deg.	$d\sigma/d\omega$ mb/str	Δ (%)	
		+	-
90.33	1.20	64.6	38.9
97.83	1.52	40.3	26.7

Avg. $d\sigma/d\omega = 1.45$ mb/str ± 25.9 %
 $\int(d\sigma/d\omega)d\omega = 18.28$ mb ± 25.9 %

$E_n = 6.00 \pm 0.00$ MeV
(n,n') to: 2.340 MeV Level

θ_{cm} deg.	$d\sigma/d\omega$ mb/str	Δ (%)	
		+	-
82.86	2.99	17.0	16.9
90.36	3.18	26.3	10.7
97.85	2.68	20.4	20.4

Avg. $d\sigma/d\omega = 3.04$ mb/str ± 11.3 %
 $\int(d\sigma/d\omega)d\omega = 38.23$ mb ± 11.3 %

$E_n = 6.00 \pm 0.00$ MeV
(n,n') to: 2.624 MeV Level
+ 2.662 MeV Level

θ_{cm} deg.	$d\sigma/d\omega$ mb/str	Δ (%)	
		+	-
82.87	10.54	8.4	7.6
90.38	10.45	9.4	7.2
97.87	10.78	9.4	8.2

Avg. $d\sigma/d\omega = 10.60$ mb/str ± 9.3 %
 $\int(d\sigma/d\omega)d\omega = 133.22$ mb ± 9.3 %

$E_n = 6.00 \pm 0.00$ MeV
(n,n') to: 3.202 MeV Level
+ 3.222 MeV Level

θ_{cm} deg.	$d\sigma/d\omega$ mb/str	Δ (%)	
		+	-
82.91	7.42	14.5	20.0
90.41	6.78	14.6	12.0
97.91	6.95	13.7	15.6

Avg. $d\sigma/d\omega = 6.96$ mb/str ± 12.0 %
 $\int(d\sigma/d\omega)d\omega = 87.47$ mb ± 12.0 %

$E_n = 6.00 \pm 0.00$ MeV
(n,n') to: 3.450 MeV Level
+ 3.600 MeV Level

θ_{cm} deg.	$d\sigma/d\omega$ mb/str	Δ (%)	
		+	-
82.93	23.71	10.8	10.0
90.44	21.80	10.1	10.6
97.94	22.66	10.1	7.5

Avg. $d\sigma/d\omega = 22.67$ mb/str ± 9.9 %
 $\int(d\sigma/d\omega)d\omega = 284.90$ mb ± 9.9 %

$E_n = 6.00 \pm 0.00$ MeV
(n,n') to: 3.776 MeV Level

θ_{cm} deg.	$d\sigma/d\omega$ mb/str	Δ (%)	
		+	-
82.97	11.34	19.1	32.2

Avg. $d\sigma/d\omega = 11.34$ mb/str ± 26.6 %
 $\int(d\sigma/d\omega)d\omega = 142.51$ mb ± 26.6 %

$E_n = 6.49 \pm 0.00$ MeV
(n,n') to: 2.340 MeV Level

θ_{cm} deg.	$d\sigma/d\omega$ mb/str	Δ (%)	
		+	-
82.85	1.92	55.3	38.4
90.35	1.14	62.3	30.0
97.86	1.02	60.5	37.0

Avg. $d\sigma/d\omega = 1.32$ mb/str $\pm 30.9\%$
 $\int(d\sigma/d\omega)d\omega = 16.54$ mb $\pm 30.9\%$

$E_n = 6.49 \pm 0.00$ MeV
(n,n') to: 3.450 MeV Level
+ 3.600 MeV Level

θ_{cm} deg.	$d\sigma/d\omega$ mb/str	Δ (%)	
		+	-
90.42	13.01	12.5	7.8
97.91	11.84	15.1	25.7

Avg. $d\sigma/d\omega = 12.79$ mb/str $\pm 10.2\%$
 $\int(d\sigma/d\omega)d\omega = 160.71$ mb $\pm 10.2\%$

$E_n = 6.49 \pm 0.00$ MeV
(n,n') to: 2.624 MeV Level
+ 2.662 MeV Level

θ_{cm} deg.	$d\sigma/d\omega$ mb/str	Δ (%)	
		+	-
82.86	7.96	11.0	11.8
90.36	6.91	23.7	13.0
97.86	6.46	18.3	9.6

Avg. $d\sigma/d\omega = 7.34$ mb/str $\pm 12.0\%$
 $\int(d\sigma/d\omega)d\omega = 92.18$ mb $\pm 12.0\%$

$E_n = 7.00 \pm 0.00$ MeV
(n,n') to: 2.624 MeV Level
+ 2.662 MeV Level

θ_{cm} deg.	$d\sigma/d\omega$ mb/str	Δ (%)	
		+	-
82.86	7.93	28.3	13.5
90.35	7.32	24.4	9.3
97.86	8.15	18.2	18.9

Avg. $d\sigma/d\omega = 7.87$ mb/str $\pm 12.6\%$
 $\int(d\sigma/d\omega)d\omega = 98.95$ mb $\pm 12.6\%$

$E_n = 6.49 \pm 0.00$ MeV
(n,n') to: 3.202 MeV Level
+ 3.222 MeV Level

θ_{cm} deg.	$d\sigma/d\omega$ mb/str	Δ (%)	
		+	-
82.89	4.66	18.1	29.4
90.39	4.43	20.3	20.7
97.89	3.39	35.9	32.2

Avg. $d\sigma/d\omega = 4.20$ mb/str $\pm 17.3\%$
 $\int(d\sigma/d\omega)d\omega = 52.71$ mb $\pm 17.3\%$

$E_n = 7.00 \pm 0.00$ MeV
(n,n') to: 3.202 MeV Level
+ 3.222 MeV Level

θ_{cm} deg.	$d\sigma/d\omega$ mb/str	Δ (%)	
		+	-
82.88	2.98	41.4	18.9
90.38	2.18	45.9	22.5

Avg. $d\sigma/d\omega = 2.79$ mb/str $\pm 19.0\%$
 $\int(d\sigma/d\omega)d\omega = 35.10$ mb $\pm 19.0\%$

$E_n = 7.00 \pm 0.00$ MeV
 (n,n') to: 3.450 MeV Level
 + 3.600 MeV Level

θ_{cm} deg.	$d\sigma/d\omega$ mb/str	Δ (%)	
		+	-
90.39	8.12	26.0	22.1

Avg. $d\sigma/d\omega = 8.12$ mb/str $\pm 25.0\%$
 $\int(d\sigma/d\omega)d\omega = 102.00$ mb $\pm 25.0\%$

$E_n = 7.00 \pm 0.00$ MeV
 (n,n') to: 3.450 MeV Level
 + 3.600 MeV Level
 + 3.776 MeV Level

θ_{cm} deg.	$d\sigma/d\omega$ mb/str	Δ (%)	
		+	-
82.89	9.77	17.6	8.5

Avg. $d\sigma/d\omega = 9.77$ mb/str $\pm 14.8\%$
 $\int(d\sigma/d\omega)d\omega = 122.78$ mb $\pm 14.8\%$

$E_n = 7.50 \pm 0.00$ MeV
 (n,n') to: 2.624 MeV Level
 + 2.662 MeV Level

θ_{cm} deg.	$d\sigma/d\omega$ mb/str	Δ (%)	
		+	-
82.85	5.46	28.7	21.3
90.35	5.72	24.5	11.4
97.85	6.31	12.8	13.4

Avg. $d\sigma/d\omega = 6.04$ mb/str $\pm 13.3\%$
 $\int(d\sigma/d\omega)d\omega = 75.93$ mb $\pm 13.3\%$

$E_n = 8.01 \pm 0.00$ MeV
 (n,n') to: 2.624 MeV Level
 + 2.662 MeV Level

θ_{cm} deg.	$d\sigma/d\omega$ mb/str	Δ (%)	
		+	-
82.84	3.92	16.0	15.9
90.34	3.00	31.7	12.8
97.84	3.74	20.4	21.9

Avg. $d\sigma/d\omega = 3.68$ mb/str $\pm 14.2\%$
 $\int(d\sigma/d\omega)d\omega = 46.23$ mb $\pm 14.2\%$

$E_n = 8.50 \pm 0.00$ MeV
 (n,n') to: 2.624 MeV Level
 + 2.662 MeV Level

θ_{cm} deg.	$d\sigma/d\omega$ mb/str	Δ (%)	
		+	-
47.75	6.89	25.1	15.0
55.28	5.64	28.5	27.1
62.80	4.75	23.1	19.5
82.84	5.45	26.4	12.8
90.34	4.09	52.5	11.5
97.84	3.70	40.9	19.1

Avg. $d\sigma/d\omega = 5.43$ mb/str $\pm 11.4\%$
 $\int(d\sigma/d\omega)d\omega = 68.20$ mb $\pm 11.4\%$

²⁰⁰Pb CROSS SECTIONS

$E_n = 6.00 \pm 0.00$ MeV
(n,n') to: 2.634 MeV Level

θ_{cm} deg.	$d\sigma/d\omega$ mb/str	Δ (%)	
		+	-
97.87	6.00	38.8	24.1
Avg. $d\sigma/d\omega = 6.00$ mb/str $\pm 32.2\%$			
$\int(d\sigma/d\omega)d\omega = 75.34$ mb $\pm 32.2\%$			

$E_n = 8.50 \pm 0.00$ MeV
(n,n') to: 2.634 MeV Level

θ_{cm} deg.	$d\sigma/d\omega$ mb/str	Δ (%)	
		+	-
47.76	7.21	33.8	13.4
55.28	4.91	49.4	17.5
62.80	5.60	40.2	17.9
Avg. $d\sigma/d\omega = 6.75$ mb/str $\pm 14.4\%$			
$\int(d\sigma/d\omega)d\omega = 84.79$ mb $\pm 14.4\%$			

$E_n = 7.00 \pm 0.00$ MeV
(n,n') to: 2.634 MeV Level

θ_{cm} deg.	$d\sigma/d\omega$ mb/str	Δ (%)	
		+	-
82.86	7.03	38.1	20.4
90.35	5.13	55.1	26.7
97.85	5.74	53.0	13.8
Avg. $d\sigma/d\omega = 6.52$ mb/str $\pm 19.5\%$			
$\int(d\sigma/d\omega)d\omega = 81.92$ mb $\pm 19.5\%$			

$E_n = 7.50 \pm 0.00$ MeV
(n,n') to: 2.634 MeV Level

θ_{cm} deg.	$d\sigma/d\omega$ mb/str	Δ (%)	
		+	-
82.85	5.88	38.9	16.9
90.35	5.72	30.0	13.0
97.85	5.41	28.7	18.8
Avg. $d\sigma/d\omega = 5.74$ mb/str $\pm 15.1\%$			
$\int(d\sigma/d\omega)d\omega = 72.12$ mb $\pm 15.1\%$			

$E_n = 8.01 \pm 0.00$ MeV
(n,n') to: 2.634 MeV Level

θ_{cm} deg.	$d\sigma/d\omega$ mb/str	Δ (%)	
		+	-
82.84	6.22	41.6	19.3
90.34	4.76	45.3	16.6
97.85	6.25	26.8	15.5
Avg. $d\sigma/d\omega = 6.08$ mb/str $\pm 13.9\%$			
$\int(d\sigma/d\omega)d\omega = 76.39$ mb $\pm 13.9\%$			



INTERNAL DISTRIBUTION

- | | |
|--|------------------------------------|
| 1-3. Central Research Library | 47-48. F. C. Maienschein |
| 4. ORNL - Y-12 Technical Library
Document Reference Section | 49. G. L. Morgan |
| 5-24. Laboratory Records Department | 50. F. R. Mynatt |
| 25. Laboratory Records, ORNL R.C. | 51. E. M. Oblow |
| 26-28. L. S. Abbott | 52. R. W. Peelle |
| 29. R. G. Alsmiller, Jr. | 53. S. K. Penny |
| 30. C. E. Clifford | 54-68. F. G. Perey |
| 31. F. L. Culler | 69. Herman Postma |
| 32. J. K. Dickens | 70. R. W. Roussin |
| 33. C. Y. Fu | 71. M. J. Skinner |
| 34. W. O. Harms | 72. R. B. Parker |
| 35. R. F. Hibbs | 73. A. Zucker |
| 36-45. W. E. Kinney | 74. H. Feshbach (Consultant) |
| 46. T. A. Love | 75. P. F. Fox (Consultant) |
| | 76. W. W. Havens, Jr. (Consultant) |
| | 77. A. F. Henry (Consultant) |

EXTERNAL DISTRIBUTION

- 78-79. USAEC Division of Reactor Research and Development, Washington, D.C. 20545
- 80. USAEC-RRD Senior Site Representative, ORNL
- 81. Research and Technical Support Division, AEC, ORO
- 82. Patent Office, AEC, ORO
- 83-309. Given distribution as shown in TID-4500 under UC-79d, Liquid Metal Fast Breeder Reactors (Physics)
- 310-369. Technical Information Center for ENDF distribution